Single-spin dynamics and decoherence in a quantum dot via charge transport

Hans-Andreas Engel* and Daniel Loss†
Department of Physics and Astronomy, University of Basel, Klingelbergstrasse 82, CH-4056 Basel, Switzerland
(Received 25 September 2001; published 14 May 2002)

We investigate the spin dynamics of a quantum dot with a spin-$\frac{1}{2}$ ground state in the Coulomb blockade regime and in the presence of a magnetic rf field leading to electron spin resonance (ESR). We show that by coupling the dot to leads, spin properties on the dot can be accessed via the charge current in the stationary and nonstationary limits. We present a microscopic derivation of the current and the master equation of the dot using superoperators, including contributions to decoherence and energy shifts due to the tunnel coupling. We give a detailed analysis of sequential and cotunneling currents, for linearly and circularly oscillating ESR fields, applied in cw and pulsed modes. We show that the sequential tunneling current exhibits a spin satellite peak whose linewidth gives a lower bound on the decoherence time T_2 of the spin-$\frac{1}{2}$ state on the dot. Similarly, the spin decoherence can be accessed also in the cotunneling regime via ESR-induced spin flips. We show that the conductance ratio of the spin satellite peak and the conventional peak due to sequential tunneling saturates at the universal conductance ratio of 0.71 for strong ESR fields. We describe a double-dot setup which generates spin-dependent tunneling and acts as a current pump (at zero bias) and as a spin inverter which inverts the spin polarization of the current, even in a homogeneous magnetic field. We show that Rabi oscillations of the dot spin induce coherent oscillations in the time-dependent current. These oscillations are observable in the time-averaged current as function of ESR pulse duration, and they allow one to access the spin coherence directly in the time domain. We analyze the measurement and readout process of the dot spin via currents in spin-polarized leads and identify measurement time and efficiency by calculating the counting statistics, noise, and the Fano factor. We point out that single spin dynamics can also be accessed with STM techniques.

DOI: 10.1103/PhysRevB.65.195321 PACS number(s): 73.63.Kv, 72.25.−b, 85.35.−p

I. INTRODUCTION

The coherent control and manipulation of the electron spin has become the focus of an increasing number of experiments.[1–8] From measurements it has become evident that the phase coherence of electron spins in semiconductors can be robust over unusually long times, exceeding hundreds of nanoseconds.[1] Thus, spins of electrons are suitable candidates for applications in the field of spintronics, in particular for quantum information processing.[9–18] This has made it desirable to understand in more detail the coherent behavior of single electron spins which are confined to nanostructures such as quantum dots, molecules, or atoms, and to point to ways of how to access the coherence time of a single spin experimentally. It is the goal of this work to address this issue and to propose and analyze transport scenarios involving a quantum dot attached to leads and with a spin-1/2 ground state.

We first remind ourselves of some basic notions in spin dynamics. When the electron spin is exposed to an external magnetic field, this leads to a Zeeman splitting, and the spin dynamics is described by the standard Bloch equations.[19] These are characterized by two time scales: the (longitudinal) relaxation time T_1 and the decoherence time T_2 (transverse relaxation). The spin relaxation time T_1 describes the lifetime of an excited spin state, aligned along the external field, and is classical in the sense that its definition does not involve the concept of quantum superpositions. Such a T_1 time of a spin in a single quantum dot was measured recently via transport and was shown to be longer than a few microseconds,[7] in agreement with calculations.[20] On the other hand, the spin decoherence time T_2 gives the time over which a superposition of opposite spin states of a single electron remains coherent. Thus, coherent manipulations of electron spins, e.g., gate operations for quantum computation, must be performed faster than T_2. We note that typically $T_2 < T_1$.[19] Thus, from the sole knowledge of T_1 no lower bound for T_2 follows. It is thus of fundamental interest to investigate possibilities of how to gain access to the decoherence time T_2 for a single spin confined to a quantum dot.

The loss of phase coherence of many but independent spins is described by the dephasing time[1] T_2^*, where inhomogeneities in the Zeeman terms lead to a further suppression of phase coherence for the ensemble but not necessarily for an individual spin, thus $T_2^* \leqslant T_2$. In recent experiments, T_2^* was measured in bulk GaAs by using ultrafast time-resolved optical methods, yielding values for T_2^* exceeding 100 ns.[1]

However, the measurement of the decoherence time T_2 for a single spin has—to our knowledge—not been reported yet (although it is expected to be within experimental reach given the known single-photon sensitivity). A first step into this direction are spin-echo measurements on an ensemble of spins, where dephasing due to inhomogeneities of the magnetic field is eliminated. Indeed, such measurements being performed more than 30 years ago on P donors in Si, reported T_2 times up to 500 μs.[21] However, it appears desirable to have a more direct method for single-spin measurements. To achieve this via direct coupling to the magnetic moment of the spin is rather challenging due to the extremely small magnetic moment, although it is believed to be within reach using cantilever techniques.[22] Here we concentrate on a further approach based on transport measurements. The key idea is to exploit the Pauli principle which connects spin and charge of the electron so intimately that all spin

properties can be accessed via charge and charge currents, especially in the Coulomb blockade regime[23] of a quantum dot attached to leads. Indeed, concrete scenarios based on such a spin-to-charge conversion have been proposed in the past,[9,11,24–26] and it is our goal here to further elaborate on these concepts and to report on a variety of new results we have obtained.

There are two classes of spin decoherence contributions we have to distinguish in the following. First, rare tunneling events of electrons onto and off the dot change the spin state on the dot and in this way contribute to the decoherence of the dot spin. We account for this decoherence microscopically in terms of a tunneling Hamiltonian. Second, there are intrinsic decoherence contributions from processes which persist even if the dot is completely isolated from the leads. This decoherence is taken into account phenomenologically in the master equation developed in this work, with an intrinsic decoherence rate T_2^{-1}. The goal then is to show that this T_2 time can be extracted via current measurements, regardless of the microscopic processes leading to T_2. Such a phenomenological approach to intrinsic decoherence makes the purpose of our considerations clearer and is applicable to different types of decoherence mechanisms, e.g., based on hyperfine and spin-orbit couplings. The microscopic study of such intrinsic decoherence, being an important subject in its own right, is not addressed in the present work.

The outline of this paper is as follows. In Sec. II, we define the system of interest, a quantum dot with spin-1/2 ground state in the Coulomb blockade regime tunnel coupled to leads and in the presence of an electron spin resonance (ESR) field. We derive the (generalized) master equation for the low-energy dot states in the sequential and cotunneling regime by evaluating the tunnel coupling to the leads microscopically in order to obtain tunneling rates, decoherence rates, and energy (Stark) shifts. For this we need to include diagonal and off-diagonal matrix elements of the reduced density operator. The stationary current through the dot and its dependence on the ESR field is discussed in Sec. III. We find a spin satellite peak in the sequential tunneling current, whose linewidth as function of the ESR frequency gives a lower bound for the T_2 time. Thus, via the stationary current, the T_2 time can be accessed in a regime that is experimentally accessible, as will be demonstrated by concrete numerical examples. We show that the ratio of this satellite peak and the main peak saturates at a universal conductance ratio for strong ESR fields. In Sec. IV, we extend our results to the even-to-odd transition, i.e., for the case where there is (on average) one electron less on the dot. In Sec. V, we explain a mechanism for a spin-inverter device which inverts the spin polarization of the current passing through two dots coupled in series in the presence of a homogeneous magnetic field. In Sec. VI, we consider rotating ESR fields which allows us to obtain the exact time evolution of the dot states and their decay rates. In Sec. VII, the cotunneling current through the quantum dot away from the sequential tunneling peak is discussed. We show that the T_2 time can also be accessed in this regime. Invoking spin-polarized leads, a readout procedure for the dot spin is proposed and analyzed in Sec. VIII, where counting statistics, noise, and the Fano factor are calculated, which allow us then to estimate the measurement time. In Sec. IX, we discuss coherent Rabi oscillations of the dot spin and their occurrence in the time-dependent current. In Sec. X, we show that Rabi oscillations can also be observed in the time-averaged current if pulsed ESR fields are applied. In Sec. XI, we point out that our results also apply to scanning tunneling microscopy (STM) devices, and we finally conclude in Sec. XII.

II. QUANTUM DOT IN ESR FIELD

A. Model Hamiltonian

We consider a quantum dot in the Coulomb blockade regime,[23] which has a spin-$\frac{1}{2}$ ground state. The dot is assumed to be tunnel coupled to two Fermi-liquid leads $l=1$, 2, at chemical potentials μ_l. We start from the full Hamiltonian

$$H=H_{\rm lead}+H_{\rm dot}+H_{\rm ESR}(t)+H_T, \tag{1}$$

which describes leads, dot, ESR field, and the tunnel coupling between leads and dot, respectively. For the leads we take $H_{\rm lead}=\Sigma_{lk\sigma}\epsilon_{lk}c^\dagger_{lk\sigma}c_{lk\sigma}$, where $c^\dagger_{lk\sigma}$ creates an electron in lead l with orbital state k, spin σ, and energy ϵ_{lk}. We describe the coupling with the standard tunnel Hamiltonian

$$H_T=\sum_{lpk\sigma} t^\sigma_{lp}c^\dagger_{lk\sigma}d_{p\sigma}+{\rm H.c.}, \tag{2}$$

with tunneling amplitude t^σ_{lp} and where $d^\dagger_{p\sigma}$ creates an electron on the dot in orbital state p. In Eq. (1), $H_{\rm dot}$ is time independent and includes charging and interaction energies of the electrons on the dot and coupling to a static magnetic field B_z in z direction. The dot spin is coupled to a magnetic ESR field, $B_x(t)=B_x^0\cos(\omega t)$, linearly oscillating in the x direction with frequency ω, thus $H_{\rm ESR}=-\frac{1}{2}g\mu_{\rm B}B_x(t)\sigma_x$. Such an oscillating field produces Rabi spin flips when its frequency is tuned to resonance, $\omega=\Delta_z$, as shown below. Then, the total Zeeman coupling of the dot spin is

$$-\frac{1}{2}g\mu_{\rm B}\mathbf{B}(t)\cdot\boldsymbol{\sigma}=-\frac{1}{2}\Delta_z\sigma_z-\frac{1}{2}\Delta_x\cos(\omega t)\sigma_x, \tag{3}$$

with electron g factor g, Bohr magneton $\mu_{\rm B}$, and Pauli matrices σ_i. We have defined $\Delta_x=g\mu_{\rm B}B_x^0$ and the Zeeman splitting $\Delta_z=g\mu_{\rm B}B_z$. Ideally, we assume that the Zeeman splitting of the leads $\Delta_z^{\rm leads}$ is different from Δ_z, and $\Delta_z^{\rm leads}\ll\varepsilon_{\rm F}$, where $\varepsilon_{\rm F}$ is the Fermi energy, such that the effects of the fields B_z and $B_x(t)$ on the leads are negligible (see below). Such a situation can be achieved by using materials of different g factors[5] and/or with local magnetic fields (B_x or B_z).

We are neglecting photon-assisted tunneling (PAT) processes,[23,27] in which oscillating electric potentials of the leads provide additional energy to electrons tunneling onto the dot. We note that PAT contributions to the current can be distinguished from ESR effects since the former contributions do not show resonant behavior as a function of B_z and/or ω, and they lead to several satellite peaks instead of one as for ESR effects (see below). Further, if one avoids

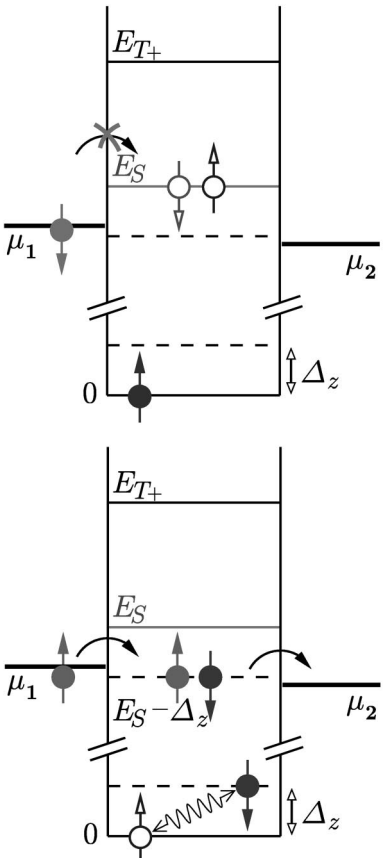

FIG. 1. Quantum dot coupled to (unpolarized) leads $l=1, 2$ with chemical potentials μ_l. The sequential tunneling regime $E_S>\mu_1>E_S-\Delta_z>\mu_2$ (for $E_\uparrow=0$) shown here corresponds to the satellite peak in the sequential tunneling current; cf. Sec. III A and III B and Figs. 2 and 3. Here, E_S (E_{T_+}) are the singlet (triplet) levels and the Zeeman splitting is $\Delta_z=g\mu_B B_z>kT$. (a) If the dot is initially in the spin ground state $|\uparrow\rangle$, sequential tunneling is blocked by energy conservation. (b) If the dot spin is excited by an ESR field (Rabi flip), spin-up electrons can tunnel from lead 1 onto the dot, forming a singlet. Then, spin-up or -down electrons can tunnel into lead 2.

electrical rf components parallel to the current, i.e., along the axis lead-dot-lead, no potential oscillations are produced, and thus PAT effects are excluded. Finally, electric rf fields can be avoided altogether, using a setup as in Ref. 28. There, the oscillating current induced in a superconducting wire (via an rf source) generates only a magnetic rf component in the near-field region,[29] with an the electric component that is negligibly small for $\omega \ll \omega_p$, where ω_p is the plasma frequency. Finally, for transport and ESR experiments in quantum Hall samples with and without quantum dots we refer to Refs. 30 and 31.

B. Dot spectrum and energetics

The electronic states of the quantum dot can be assumed as follows. For an odd number N of electrons on a dot with antiferromagnetic filling, the dot has a spin-$\frac{1}{2}$ ground state. The topmost (excess) electron can be either in the spin ground state $|\uparrow\rangle$ (σ_z eigenstate) or in the excited state $|\downarrow\rangle$ (see Fig. 1). This assumption is automatically satisfied if $N=1$. Otherwise, to obtain antiferromagnetic filling, Hund's rule must not apply. This can be achieved by breaking the orbital degeneracy on the dot, e.g., by using asymmetrically shaped dots or an appropriate magnetic field B_z.[32] For an additional electron on the dot, we assume for $N+1$ the ground state to be the singlet $|S\rangle=(|\uparrow\downarrow\rangle-|\downarrow\uparrow\rangle)/\sqrt{2}$; i.e., the triplet state $|T_+\rangle=|\uparrow\uparrow\rangle$ has higher energy, which again can be achieved by tuning B_z.[32] The energy E_m of the dot, including charging energy, is defined by $H_{\rm dot}|m\rangle=E_m|m\rangle$.

We shall give a brief overview of the energetics involved in tunneling through quantum dots in the Coulomb blockade regime[23] and in the presence of the Zeeman splitting and an ESR field. For simplicity, we assume that there is no electron-electron interaction on the dot apart from the classical charging effect. (Our work is not restricted to such an assumption, since we only require a spin-$\frac{1}{2}$ ground state and a large enough singlet-triplet spacing on the dot.) The total ground-state energy of a dot with antiferromagnetic filling is

$$U(N)=\sum_{k=1}^{N}\varepsilon_k^\sigma+E_C^N, \tag{4}$$

for N electrons on the dot. Here, the single-particle energy of the kth electron, $\varepsilon_k^\sigma=\varepsilon_k+(-1)^k\Delta_z/2$, contains orbital and Zeeman energy contributions. The charging energy is $E_C^N=(Ne-Q_G)^2/2C$, with gate charge Q_G, and dot capacitance C. It is convenient to define the chemical potential of the dot, $\mu_{\rm dot}(N+1)=U(N+1)-U(N)$, which is the energy required for an electron of lead l to tunnel onto the dot, which contains N electrons initially, i.e., tunneling onto the dot occurs for $\mu_l>\mu_{\rm dot}$.[33] In the Coulomb blockade regime, $kT \ll e^2/C$ (k: Boltzmann constant), no sequential tunneling current flows through the dot if the chemical potentials of dot and leads are such that $\mu_{\rm dot}(N)<\mu_1$, $\mu_2<\mu_{\rm dot}(N+1)$. However, in the sequential tunneling regime $\mu_1>\mu_{\rm dot}(N+1)>\mu_2$, single electrons tunnel from lead 1 onto the dot and then on into lead 2, producing a sequential tunneling current.

In the presence of an ESR field, these concepts must be extended. Excitations of the dot states must be taken into account, since now the energy of the dot changes in time due to $B_x(t)$. A full analytical description of the current flow is derived in the following sections based on a time-dependent master equation. Here, we just intend to give a qualitative picture to provide some intuition for the underlying physical mechanism (it will not be needed later on). We define a time-dependent chemical potential of the dot, given as the energy required to add an electron at time t. We consider the two chemical potentials $\mu_{\rm dot}^\sigma$ for initial spin-$\frac{1}{2}$ dot state $|\sigma\rangle$, i.e., $\Delta_{S\uparrow}=\mu_{\rm dot}^\uparrow(N+1)=E_S-E_\uparrow$ and $\Delta_{S\downarrow}=\mu_{\rm dot}^\uparrow(N+1)=E_S-E_\downarrow$, which simplify to $\Delta_{S\uparrow}=E_S$, and $\Delta_{S\downarrow}=E_S-\Delta_z$, respectively, for $E_\uparrow=0$. Note that the $\mu_{\rm dot}^\sigma$ is *lowered* if the dot is excited into state $|\downarrow\rangle$, since the Zeeman energy Δ_z has already been provided by a Rabi spin flip due to the ESR field. Therefore, we can identify the regime $\Delta_{S\uparrow}>\mu_1>\Delta_{S\downarrow}>\mu_2$, where a sequential tunneling current will flow through the dot only after exciting the dot spin by a spin flip (see Fig. 1). In other words, the dot can be opened and closed via the

ESR field, which thus allows one to modulate the current. This (dynamical) dependence of the current on the dot spin can be exploited to measure the T_2 time and the Rabi oscillations of the dot spin,[25] as we will explain in detail in the following.

C. Systematic treatment of sequential tunneling

The electronic states on a quantum dot interact with their environment (heat bath), in particular with the Fermi leads, which provide and take up electrons. The state of the combined system, dot and environment, is given by the full density matrix $\rho(t)$. The states of interest are the electronic states on the dot, described by the reduced density matrix of the dot, $\rho_{\rm D}=\mathrm{Tr}_{\rm B}\rho$. Here, $\mathrm{Tr}_{\rm B}$ is the trace taken over the leads (environment), averaging over the (unobserved) degrees of freedom of the environment. The diagonal elements $\rho_n=\langle n|\rho_{\rm D}|n\rangle$ of the density matrix of the dot describe the occupation probabilities of the dot levels, with $H_{\rm dot}|n\rangle=E_n|n\rangle$. The off-diagonal elements $\rho_{nm}=\langle n|\rho_{\rm D}|m\rangle=\rho_{mn}^*$ describe the coherence and the phase of superpositions of dot states.

The tunnel coupling H_T between leads and dot is switched on at $t=0$. Prior to this, the dot and leads are assumed to be uncorrelated such that the full initial density matrix factorizes as $\rho(0)=\rho_{\rm D}(0)\rho_{\rm B}^0$, where $\rho_{\rm B}^0$ is the density matrix of the leads in thermal equilibrium at $\mu_{1,2}$, and at temperature T. Next we derive the master equation for the reduced density matrix $\rho_{\rm D}$ by making use of the superoperator formalism.[34] In the following, we set $\hbar=1$. Starting from the von Neumann equation $\dot\rho=-i[H,\rho]$ for the full density matrix and using standard manipulations,[34] one finds the time evolution of the reduced density matrix

$$\dot\rho_{\rm D}(t)=-i[H_{\rm dot}+H_{\rm ESR}(t),\rho_{\rm D}(t)]-\int_0^t dt' M(t,t')\rho_{\rm D}(t'), \tag{5}$$

$$M(t,t')=\mathrm{Tr}_{\rm B}L_T(\mathcal{T}e^{-i\int_{t'}^t dt'' QL(t'')})L_T\rho_{\rm B}^0, \tag{6}$$

with time ordering $\mathcal{T}$ and the Liouville operators defined by $L(t)X=[H(t),X]$, $L_TX=[H_T,X]$, and equivalently for $L_{\rm dot}$, $L_{\rm lead}$, and $L_{\rm ESR}(t)$. The projectors are defined as $Q=1-P$ and $PX=\rho_{\rm B}^0\mathrm{Tr}_{\rm B}X$. The kernel M [Eq. (6)] is a superoperator describing processes involving tunneling of electrons to and from the leads. We consider here only sequential tunneling processes and refer for a discussion of cotunneling contributions to Secs. II F and VII. Thus, we work in Born approximation by retaining only the terms in lowest order of L_T; i.e., we replace L by $L_0=L-L_T$ in Eq. (6). For further evaluation of M, it is self-consistent (see below) to neglect the effect of the ESR field, $L_{\rm ESR}(t)$; i.e., we replace L_0 by $L_{\rm dot}+L_{\rm lead}$ in M. This removes explicitly the time dependence of M, making it time translation invariant, $M(t,t')=M(t-t')$. We find that $M(\tau)$ decays on a time scale $\tau_c\sim 1/kT$, i.e., the correlations induced in the leads by H_T decay rapidly. Since this decay is typically much faster than the Rabi flips produced by the ESR field, $\tau_c\ll 1/\Delta_x$, we may indeed neglect the contribution of $L_{\rm ESR}(t)$ to M. With these approximations, Eq. (5) becomes in the interaction picture

$$\dot\rho_{\rm D}^{\rm I}(t)=-iL_{\rm ESR}^{\rm I}(t)\rho_{\rm D}^{\rm I}(t)-\int_0^t d\tau M^{\rm I}(\tau)\rho_{\rm D}^{\rm I}(t-\tau). \tag{7}$$

The rapid decay of $M(\tau)$ also justifies the Markovian assumption that the system has no memory about its past, i.e., that $\dot\rho_{\rm D}(t)$ depends only on $\rho_{\rm D}(t)$ and not on $\rho_{\rm D}(t-\tau)$. This approximation is performed in the interaction picture, to keep track of the dynamical phase of the off-diagonal elements of $\rho_{\rm D}$. Systematically we proceed as follows. Since the integrand in Eq. (7) only contributes for small τ, we may expand the integrand in τ, $M(\tau)\rho_{\rm D}^{\rm I}(t-\tau)=M(\tau)[\rho_{\rm D}^{\rm I}(t)-\tau\dot\rho_{\rm D}^{\rm I}(t)+O(\tau^2)]$. We then replace $\dot\rho_{\rm D}^{\rm I}(t)$ in the integrand by using Eq. (7) iteratively. However, since $M(\tau)\sim O(L_T^2)$, we can neglect the part of $\dot\rho_{\rm D}^{\rm I}(t)$ which is $O(L_T^2)$, since it corresponds to a higher-order term in our Born approximation. The remaining part of $\dot\rho_{\rm D}^{\rm I}(t)$ results from $L_{\rm ESR}$, which can also be disregarded since, in the integrand, the ESR field only acts on the time scale $\tau_c\ll 1/\Delta_x$. We then extend the upper integration limit in Eq. (7) to ∞, with negligible contributions due to the decay of $M(\tau)$. Therefore, the second term in Eq. (7) becomes $-\{\int_0^\infty d\tau M^{\rm I}(\tau)\}\rho_{\rm D}^{\rm I}(t)$. Next, we evaluate the matrix elements $M_{bc|nm}=\langle b|(M|n\rangle\langle m|)|c\rangle$ explicitly in the interaction picture, which yields[35]

$$\begin{aligned}-\int_0^\infty d\tau M_{bc|nm}^{\rm I}(\tau)=\delta_{bc}\delta_{nm}&\Big(W_{cn}-\delta_{bn}\sum_k W_{kn}\Big)\\&-(1-\delta_{nm})\delta_{bn}\delta_{mc}\\&\times\Big[i\delta\epsilon_{nm}+\frac{1}{2}\sum_k (W_{kn}+W_{km})\Big],\end{aligned} \tag{8}$$

with the rates W (see below) and energy shifts $\delta\epsilon_{nm}$ (Stark shifts). These shifts are small; e.g., the one between $|\downarrow\rangle$ and $|\uparrow\rangle$ is given by

$$\delta\epsilon_{\downarrow\uparrow}=\frac{1}{2\pi}\sum_l \mathcal{P}\int_0^\infty d\epsilon f_l(\epsilon)\Big(\frac{\gamma_l^\uparrow}{\epsilon-\Delta_{S\downarrow}}-\frac{\gamma_l^\downarrow}{\epsilon-\Delta_{S\uparrow}}\Big), \tag{9}$$

and similarly for $\delta\epsilon_{S\downarrow}$ and $\delta\epsilon_{S\uparrow}$. For $|\mu_l-\Delta_{S\sigma}|>kT$, the energy shift becomes

$$\delta\epsilon_{\downarrow\uparrow}=\sum_l\Big(\frac{\gamma_l^\downarrow}{2\pi}\ln\Big|\frac{\Delta_{S\uparrow}}{\mu_l-\Delta_{S\uparrow}}\Big|-\frac{\gamma_l^\uparrow}{2\pi}\ln\Big|\frac{\Delta_{S\downarrow}}{\mu_l-\Delta_{S\downarrow}}\Big|\Big), \tag{10}$$

which, for $\gamma_l^\uparrow=\gamma_l^\downarrow$, reduces to $\delta\epsilon_{\downarrow\uparrow}\approx\Sigma_l(\gamma_l/2\pi)\ln[|\mu_l-\Delta_{S\downarrow}|/|\mu_l-\Delta_{S\uparrow}|]$ and, thus, to a small correction $|\delta\epsilon_{\downarrow\uparrow}|\lesssim\gamma\ln(\Delta_z/kT)$, for $\Delta\mu<\Delta_z$.

The sequential tunneling rates in Eq. (8) are

$$W_{S\downarrow}=\sum_l W_{S\downarrow}^l,\quad W_{S\downarrow}^l=\gamma_l^\uparrow f_l(\Delta_{S\downarrow}), \tag{11}$$

$$W_{\downarrow S}=\sum_l W^l_{\downarrow S}, \quad W^l_{\downarrow S}=\gamma^{\uparrow}_l[1-f_l(\Delta_{S\downarrow})], \tag{12}$$

with the Fermi function $f_l(\Delta_{S\downarrow})=[1+e^{(\Delta_{S\downarrow}-\mu_l)/kT}]^{-1}$ of lead l. The rates $W_{S\uparrow}$, $W_{\uparrow S}$, $W^l_{S\uparrow}$, and $W^l_{\uparrow S}$ are defined analogously as functions of $\gamma^{\downarrow}_l$ and $f_l(\Delta_{S\uparrow})$, and $W_{nn}=0$. The transition rates

$$\gamma^{\uparrow}_l=2\pi\nu_{\uparrow}|t^{\uparrow}_l|^2, \quad \gamma^{\downarrow}_l=2\pi\nu_{\downarrow}|t^{\downarrow}_l|^2 \tag{13}$$

consist of (possibly) spin-dependent densities of states $\nu_{\uparrow,\downarrow}$ at the Fermi energy and tunneling amplitude $t^{\uparrow,\downarrow}_l$. (Spin-dependent densities of states are considered in Sec. VIII for spin readout.) For later convenience, we define for $\sigma=\uparrow,\downarrow$

$$\gamma^{\sigma}=(\gamma^{\sigma}_1+\gamma^{\sigma}_2)/2, \quad \gamma=(\gamma^{\uparrow}+\gamma^{\downarrow})/2. \tag{14}$$

D. Master equation

So far we have considered only coupling to an environment consisting of Fermi leads. However, the electronic dot states are affected also by intrinsic degrees of freedom such as hyperfine coupling, spin-orbit interaction, or spin-phonon coupling, which lead to intrinsic spin relaxation and decoherence. Treating such couplings microscopically is beyond the present scope (see, e.g., Ref. 20). Thus, we treat these couplings phenomenologically by introducing corresponding rates in the master equation. First, the spin *relaxation* rates $W_{\uparrow\downarrow}$ and $W_{\downarrow\uparrow}$ describe processes in which the dot spin is flipped. We can assume $W_{\uparrow\downarrow}\gg W_{\downarrow\uparrow}$, for $\Delta_z>kT$ (consistent with detailed balance, $W_{\uparrow\downarrow}/W_{\downarrow\uparrow}=e^{\Delta_z/kT}$). These relaxation processes correspond to the phenomenological rate $1/T_1=W_{\uparrow\downarrow}+W_{\downarrow\uparrow}$; see also Sec. II E. Second, the rate $1/T_2$ describes the intrinsic *decoherence* of the spin on the dot, which is present even in the absence of coupling to the leads. This type of decoherence destroys the information about the relative phase in a superposition of $|\uparrow\rangle$ and $|\downarrow\rangle$, without changing the populations of the opposite spin states. Formally, this leads to a decay of the off-diagonal matrix element $\rho_{\downarrow\uparrow}$. Including the decoherence contribution of H_T [Eqs. (8) and (11)], the total spin decoherence rate is

$$V_{\downarrow\uparrow}=\frac{W_{S\uparrow}+W_{S\downarrow}}{2}+\frac{1}{T_2}; \tag{15}$$

i.e., electrons tunneling onto the dot further destroy spin coherence on the dot (see Sec. II E for an interpretation).

With the above results, we obtain from Eq. (5) the master equation of the dot,

$$\dot{\rho}_{\uparrow}=-(W_{\downarrow\uparrow}+W_{S\uparrow})\rho_{\uparrow}+W_{\uparrow\downarrow}\rho_{\downarrow}+W_{\uparrow S}\rho_S -\Delta_x\cos(\omega t)\,\mathrm{Im}[\rho_{\downarrow\uparrow}], \tag{16}$$

$$\dot{\rho}_{\downarrow}=W_{\downarrow\uparrow}\rho_{\uparrow}-(W_{\uparrow\downarrow}+W_{S\downarrow})\rho_{\downarrow}+W_{\downarrow S}\rho_S+\Delta_x\cos(\omega t)\,\mathrm{Im}[\rho_{\downarrow\uparrow}], \tag{17}$$

$$\dot{\rho}_S=W_{S\uparrow}\rho_{\uparrow}+W_{S\downarrow}\rho_{\downarrow}-(W_{\uparrow S}+W_{\downarrow S})\rho_S, \tag{18}$$

$$\dot{\rho}_{\downarrow\uparrow}=-i\Delta_z\rho_{\downarrow\uparrow}+i\frac{\Delta_x}{2}\cos(\omega t)(\rho_{\uparrow}-\rho_{\downarrow})-V_{\downarrow\uparrow}\rho_{\downarrow\uparrow}, \tag{19}$$

$$\dot{\rho}_{S\uparrow}=-i\Delta_{S\uparrow}\rho_{S\uparrow}-V_{S\uparrow}\rho_{S\uparrow}, \tag{20}$$

$$\dot{\rho}_{S\downarrow}=-i\Delta_{S\downarrow}\rho_{S\downarrow}-V_{S\downarrow}\rho_{S\downarrow}. \tag{21}$$

Here, the time evolution of the matrix elements $\rho_{nm}=\langle n|\rho_{\mathrm{D}}|m\rangle$ of the density matrix of the dot is described for the states $|n\rangle=|\uparrow\rangle$, $|\downarrow\rangle$, $|S\rangle$; e.g., for the diagonal element we write $\rho_{\uparrow}=\langle\uparrow|\rho_{\mathrm{D}}|\uparrow\rangle$, for the off-diagonal element, $\rho_{S\uparrow}=\langle S|\rho_{\mathrm{D}}|\uparrow\rangle$, etc. The rate W_{mn} describes transitions from state $|n\rangle$ to $|m\rangle$. Equations (16)–(18) are rate equations with gain and loss terms, up to the contributions from the ESR field. Then, the population of, say, state $|\uparrow\rangle$ is changed by $d\rho_{\uparrow}$ after time dt by the following contributions [Eq. (16)]. The population $\rho_{\uparrow}$ is increased when the dot is previously in state $|S\rangle$ (with probability ρ_S), and a spin $\downarrow$ electron tunnels out of the dot with probability $W_{\uparrow S}dt$. However, the population $\rho_{\uparrow}$ is decreased when the system was already in state $|\uparrow\rangle$, and a spin $\downarrow$ electron tunnels onto the dot with probability $W_{S\uparrow}dt$. The spin-flip rates $W_{\uparrow\downarrow}$ and $W_{\downarrow\uparrow}$ enter Eq. (16) analogously. In the absence of an ESR field, the off-diagonal elements [Eqs. (19)–(21)] of the density matrix decouple from the diagonal ones and decay with the decoherence rates $V_{nm}=V_{mn}$.

In the presence of an ESR field, the diagonal [Eqs. (16) and (17)] and the off-diagonal [Eq. (19)] matrix elements become coupled by the term proportional to Δ_x. This coupling of populations ($\rho_{\uparrow}$ and $\rho_{\downarrow}$) and coherence ($\rho_{\downarrow\uparrow}$) shows the coherent nature of Rabi spin flips and makes it apparent that we are studying a resonant process, which requires that we take H_{ESR} fully into account.

The current $I_2=e\langle dq/dt\rangle$ from the dot into lead 2 is defined by the number of charges dq that accumulate in lead 2 after time dt. With probability ρ_S, the dot is in state $|S\rangle$ and a charge e will tunnel into lead 2 with probability $(W^2_{\uparrow S}+W^2_{\downarrow S})dt$. However, if the dot is in state $|\uparrow\rangle$ or $|\downarrow\rangle$, a charge may tunnel from lead 2 onto the dot, reducing the number of charges in lead 2. Thus, in total we obtain for the current in lead 2

$$I_2=e(W^2_{\uparrow S}+W^2_{\downarrow S})\rho_S-eW^2_{S\uparrow}\rho_{\uparrow}-eW^2_{S\downarrow}\rho_{\downarrow}. \tag{22}$$

The current in lead 1, I_1, is obtained analogously and is given by Eq. (22) after changing sign and replacing the index 2 by 1. We show in Sec. III that $I_1=I_2$ in the stationary limit, due to charge conservation.

Finally we note that Eqs. (20) and (21), which describe a superposition of an odd and an even number of electrons on the dot, decouple from Eqs. (16)–(19) and are thus not of relevance for our considerations. Further, since the coupling to the leads is switched on only at $t=0$, initially the number of particles on the dot is well defined. Therefore $\rho_{S\uparrow}$ and $\rho_{S\downarrow}$ vanish at $t=0$ and at all later times, as seen from Eqs. (20) and (21). In particular, no superposition of a state with an even and a state with an odd number of electrons on the dot is produced by the coupling to the leads, since this would require a coherent superposition of corresponding states in

the leads; however, for times larger than τ_c (which is typically the case), we can safely neglect any coherence in the Fermi-liquid leads.

E. Decoherence and measurement process

We elucidate the connection between spin decoherence and measurement, first in the absence of leads and ESR field. We consider a coherent superposition $\alpha|\uparrow\rangle+\beta|\downarrow\rangle$ as the initial state of the dot. This pure state corresponds to the reduced density matrix $\rho_\uparrow(0)=|\alpha|^2$, $\rho_\downarrow(0)=|\beta|^2$, and $\rho_{\downarrow\uparrow}(0)=\alpha^*\beta$, and the master equation contains only the rates $W_{\uparrow\downarrow}$, $W_{\downarrow\uparrow}$, and $V_{\downarrow\uparrow}=1/T_2$. The off-diagonal terms $\rho_{\downarrow\uparrow}=\rho_{\uparrow\downarrow}^*$, decay with the decoherence time T_2, $\rho_{\downarrow\uparrow}(t)=e^{-t/T_2-it\Delta_z}\rho_{\downarrow\uparrow}(0)$, while the diagonal terms (occupation probabilities) decay with the spin relaxation time $T_1=(W_{\uparrow\downarrow}+W_{\downarrow\uparrow})^{-1}$ and $\rho_\downarrow(t)=\rho_\downarrow^{\rm eq}+e^{-t/T_1}[\rho_\downarrow(0)-\rho_\downarrow^{\rm eq}]$ toward their stationary value $\rho_\downarrow^{\rm eq}=W_{\downarrow\uparrow}/(W_{\uparrow\downarrow}+W_{\downarrow\uparrow})$ and $\rho_\uparrow=1-\rho_\downarrow$. In total, for $T_2<T_1$, we can picture the decay of $\rho_{\rm D}$ as

$$\begin{pmatrix} |\alpha|^2 & \alpha\beta^* \\ \alpha^*\beta & |\beta|^2 \end{pmatrix} \overset{T_2}{\to} \begin{pmatrix} |\alpha|^2 & 0 \\ 0 & |\beta|^2 \end{pmatrix} \overset{T_1}{\to} \begin{pmatrix} \rho_\uparrow^{\rm eq} & 0 \\ 0 & \rho_\downarrow^{\rm eq} \end{pmatrix}; \quad (23)$$

i.e., the off-diagonal terms vanish first on the time scale T_2, and then the diagonal ones equilibrate on the time scale T_1.

As shown in Sec. II C, when electrons tunnel onto the dot, the decoherence rate $V_{\downarrow\uparrow}$ [Eq. (15)] and thus the decay of the off-diagonal elements are increased further. We note now the formal equivalence to the quantum measurement process (in the σ_z basis), where the dot spin is projected onto $|\uparrow\rangle$ or $|\downarrow\rangle$, and thus the off-diagonal matrix elements vanish. This projection can be understood as a decoherence process. Conversely, we can consider the decoherence due to tunneling as a measurement performed by the tunneling electrons. We note that this process is a *weak* measurement in the following sense. The electrons in the leads attempt to tunnel on the dot, but only with small probability $\propto W_{S\sigma}$ are these attempts successful. Thus, the current I, which carries away the information of the dot state to the observer, is formed by these successful electrons, while the unsuccessful electrons are not detected. Another way to say this is that a given electron from the lead has only a small probability $\propto W_{S\sigma}$ to "measure" (i.e., decohere) the dot state.

F. Cotunneling contribution to the sequential tunneling regime

We work in the sequential tunneling regime, defined by $\mu_1>\Delta_{S\downarrow}>\mu_2$. One can see that higher-order—cotunneling—contributions can be neglected[23,24] for $\gamma_l<\Delta_z, kT$, and $\Delta\mu<\Delta_z$, the regime of interest here. Most importantly, the cotunneling contributions to $V_{\downarrow\uparrow}$ are of the order γ_l^2/Δ_z (see Sec. VII); i.e., they are suppressed compared to the sequential tunneling contributions by a factor of γ_l/Δ_z ($\approx 5\times10^{-5}$ for the parameters of Fig. 3). Formally, the cotunneling contributions to the master equation can be absorbed into T_1 and T_2. For a discussion of cotunneling currents away from the sequential tunneling resonance see Sec. VII.

III. STATIONARY CURRENT

We now consider the stationary current I in the presence of a continuous-wave (cw) ESR field. Therefore we calculate the stationary solution $\rho(t\to\infty)$ of the master equation [Eqs. (16)–(21)]. We will apply the rotating-wave approximation (RWA),[36] where only the leading frequency contributions of $H_{\rm ESR}$ are retained. Higher-order contributions would include the simultaneous absorption of two photons and the emission of another photon. In lowest order, only single photons can be absorbed or emitted, producing a spin flip on the dot. To perform this approximation, we write $\Delta_x\cos(\omega t)=\frac{1}{2}\Delta_x(e^{i\omega t}+e^{-i\omega t})$; i.e., we decompose the linearly oscillating magnetic field into a superposition of a clockwise and an anticlockwise rotating field. Integrating Eqs. (16), (17), and (19), one finds that for $\omega\approx\Delta_z$, the anticlockwise rotating field leads to rapidly oscillating terms in the integrands, which nearly average to zero. Therefore, we retain only the clockwise rotating field, which is given by the term proportional to $e^{i\omega t}$ (see also Sec. VI). Note that since only one field component contributes, the field amplitude is halved. This leads to the period T_Ω of one Rabi oscillation,

$$T_\Omega=\frac{4\pi}{\Delta_x}. \quad (24)$$

The RWA is valid for Δ_x, $V_{\downarrow\uparrow}$, $|\Delta_z-\omega|\ll\omega$ (see, e.g., Ref. 37) and is well justified for the parameters considered here. In the stationary case and using the RWA, the dependence of $\rho_\uparrow$ and $\rho_\downarrow$ [Eqs. (16) and (17)] on $\rho_{\downarrow\uparrow}$ is eliminated, leading to the effective spin-flip rate

$$W_\omega=\frac{\Delta_x^2}{8}\frac{V_{\downarrow\uparrow}}{(\omega-\Delta_z)^2+V_{\downarrow\uparrow}^2}, \quad (25)$$

which is a Lorentzian as a function of ω with maximum $W_\omega^{\max}=\Delta_x^2/8V_{\downarrow\uparrow}$ at resonance $\omega=\Delta_z$.

Now it is straightforward to find the stationary solution of the effective rate equations for $\rho_\uparrow$, $\rho_\downarrow$ and ρ_S,

$$\rho_\uparrow=\eta[W_{\uparrow S}W_{S\downarrow}+(W_{\uparrow\downarrow}+W_\omega)(W_{\uparrow S}+W_{\downarrow S})], \quad (26)$$

$$\rho_\downarrow=\eta[W_{\downarrow S}W_{S\uparrow}+(W_{\downarrow\uparrow}+W_\omega)(W_{\uparrow S}+W_{\downarrow S})], \quad (27)$$

$$\rho_S=\eta[W_{S\uparrow}W_{S\downarrow}+W_{S\uparrow}(W_{\uparrow\downarrow}+W_\omega)+W_{S\downarrow}(W_{\downarrow\uparrow}+W_\omega)], \quad (28)$$

where the normalization factor η is such that $\Sigma_n\rho_n=1$. We see from Eqs. (26)–(28) that the effective spin-flip rates are $W_{\uparrow\downarrow}+W_\omega$ and $W_{\downarrow\uparrow}+W_\omega$; i.e., the ESR field flips up and down spin with equal rate W_ω.

We can now calculate the spin-$\uparrow$ polarized current in lead 2, $I_2^\uparrow=eW_{\downarrow S}^2\rho_S-eW_{S\downarrow}^2\rho_\downarrow$ [cf. Eq. (22)]. The result is displayed in Eq. (A1) in the Appendix. The spin-$\downarrow$ polarized current $I_2^\downarrow$ is obtained from Eq. (A1) by interchanging $\uparrow$ with $\downarrow$ in the numerator (the denominator remains unaffected by such an interchange). The currents in lead 1, $I_1^{\uparrow,\downarrow}$, are obtained from the formulas for $I_2^{\uparrow,\downarrow}$ by changing sign and interchanging indices 1 with 2. Note that generally $I_1^\uparrow\neq I_2^\uparrow$, since the ESR field generates spin flips on the dot, and thus the

spin on the dot is not a conserved quantity. However, the stationary charge current $I_l=\Sigma_\sigma I_l^\sigma$ is the same in both leads, $I=I_1=I_2$, due to charge conservation.

A. Spin satellite peak

In this subsection we discuss the stationary current I through the dot, in particular, its behavior as function of $\mu=(\mu_1+\mu_2)/2$ or, equivalently, as a function of the gate voltage V_g. We will see that an additional sequential tunneling peak (satellite peak) will appear due to the ESR field. Before explicit evaluation of the current, we briefly describe this situation in qualitative terms. We assume a large Zeeman splitting $\Delta_z>\Delta\mu,kT$, with applied bias $\Delta\mu=\mu_1-\mu_2>0$. If the potentials are such that $\mu_1>\Delta_{S\uparrow}>\mu_2$—i.e., the chemical potential of the dot (relative to the ground state $|\uparrow\rangle$) is between the chemical potentials of the leads—the state of the dot changes between $|\uparrow\rangle$ and $|S\rangle$ due to sequential tunneling events, leading to the standard sequential tunneling peak in $I(\mu)$ at $\mu\approx\Delta_{S\uparrow}$.

However, we also have to consider the regime $\Delta_{S\uparrow}>\mu_1>\Delta_{S\downarrow}>\mu_2$, as shown in Fig. 1. Without an ESR field, the dot relaxes into its ground state $|\uparrow\rangle$ (since $W_{\downarrow\uparrow}\ll W_{\uparrow\downarrow}$), and the sequential tunneling current through the dot is blocked since the chemical potential $\Delta_{S\uparrow}$ of the dot is higher than those of the leads. However, if an ESR field generates Rabi spin flips (on the dot only), the current flows through the dot involving the state $|\downarrow\rangle$, since $\Delta_{S\downarrow}$ is lower than μ_1. Therefore, a sequential tunneling current appears also for gate voltages V_g corresponding to $\Delta_{S\downarrow}$; i.e., $I(\mu)$ exhibits a spin satellite peak due to the ESR field at $\mu\approx\Delta_{S\downarrow}$. This new peak is shifted away from the main peak by Δ_z (Fig. 2). The presence of such a satellite peak and its sensitivity to changes in B_z allows identification of spin effects.[38] Further, we note that via the position of the peak in $I(\omega)$, $I(B_z)$, or $I(\mu)$, the Zeeman splitting and also the g factor of a single dot can be measured. Such a measurement could provide a useful technique to study g-factor-modulated materials, where the g factor can be controlled by shifting the equilibrium position of the electrons in the dot from one layer to another by electrical gating.[11] Note that measurement of the peak position would also allow to access the Stark shifts [Eq. (9)]. We consider now the analytic expression for the current I, as given in Eq. (A1), for the regime of the spin satellite peak. In this regime, $\Delta_{S\uparrow}-\mu_1=\Delta_{S\downarrow}+\Delta_z-\mu_2-\Delta\mu>\Delta_z-\Delta\mu\approx\Delta_z>kT$, and thus $f_l(\Delta_{S\uparrow})=0$, $W_{S\uparrow}^l=0$, and $W_{\uparrow S}^l=\gamma_l^\downarrow$. For simplicity, we consider $\gamma_l=\gamma_l^\uparrow=\gamma_l^\downarrow$ here (cf. the Appendix for pumping due to $\gamma_l^\uparrow\neq\gamma_l^\downarrow$). The expression for the stationary current [Eq. (A1)] considerably simplifies to

$$I(\omega,\mu)=2e(W_{\downarrow\uparrow}+W_\omega)\gamma_1\gamma_2[f_1(\Delta_{S\downarrow})-f_2(\Delta_{S\downarrow})]\times\{(2\gamma-W_{\uparrow\downarrow}-W_\omega)[\gamma_1 f_1(\Delta_{S\downarrow})+\gamma_2 f_2(\Delta_{S\downarrow})]+4\gamma(W_{\uparrow\downarrow}+W_{\downarrow\uparrow}+2W_\omega)\}^{-1}. \quad (29)$$

For a plot of I vs ω and μ and some explanations of its characteristics, see Fig. 2.

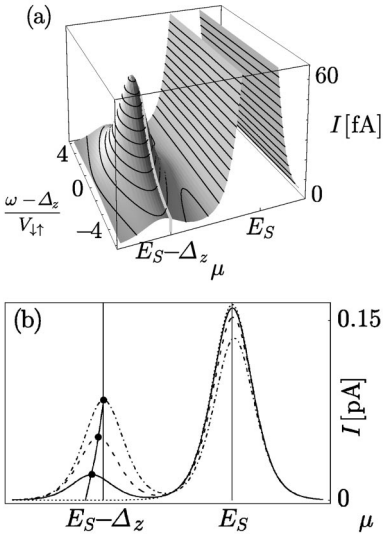

FIG. 2. The stationary current I [Eq. (A1)] vs $\mu=(\mu_1+\mu_2)/2$ and ESR frequency ω. We take $T=70$ mK, $\Delta\mu/e=6$ μV, $B_z=0.5$ T, $g=2$, $T_1=1$ μs, $T_2=100$ ns, $\gamma_1=5\times10^6$ s^{-1}, and $\gamma_2=5\gamma_1$, i.e., $\Delta_z=10kT$ and $\Delta\mu=kT$. The width of the sequential tunneling peaks in $I(\mu)$ is determined by the temperature; see Eq. (31). (a) The current $I(\mu,\omega)$ shows a spin satellite peak near $\mu=E_S-\Delta_z$ (for $E_\uparrow=0$) due to the ESR field. Note that the spin satellite peak is slightly shifted from this position [see Eq. (35)], which is indicated by the line at $E_S-\Delta_z$ (light gray line) in (a). Here, $B_x^0=1.4$ G, i.e., $W_\omega^{\max}=\gamma_1$ at resonance and $\mu=\Delta_{S\downarrow}$. (b) The current $I(\mu)$ for $W_\omega=0$ (dotted line), $\gamma_1/5$ (solid line), γ_1 (dashed line), and $9\gamma_1$ (dash-dotted line). The position of the spin satellite peak as function of W_ω is shown as black dots and the connecting solid line.

B. Spin decoherence time T_2

Around the spin satellite peak, it is possible to measure W_ω via the current and thereby access the spin decoherence time of the spin-$\frac{1}{2}$ state on the dot. For this, we identify a regime where the Rabi spin flips on the dot become the bottleneck for electron transport through the quantum dot such that the current becomes proportional to the spin-flip rate W_ω. For $kT<\Delta\mu$ and $W_\omega^{\max}<\max\{W_{\uparrow\downarrow},\gamma_1\}$ we obtain for the stationary current [Eq. (29)]

$$I(\omega)=\frac{2e\gamma_1\gamma_2(W_{\downarrow\uparrow}+W_\omega)}{\gamma_1(\gamma_1+\gamma_2)+W_{\uparrow\downarrow}(\gamma_1+2\gamma_2)}; \quad (30)$$

see Fig. 3. We have used $W_{\downarrow\uparrow}<W_{\uparrow\downarrow}$ here. In the linear response regime $kT>\Delta\mu$ and for $W_\omega^{\max}<\max\{W_{\uparrow\downarrow},\gamma f_1(\Delta_{S\downarrow}+\Delta\mu/2)\}$, the current is

$$I(\omega)=\frac{e\gamma_1\gamma_2(W_{\downarrow\uparrow}+W_\omega)\Delta\mu}{2(\gamma_1+\gamma_2)kTh(T)}\cosh^{-2}\left(\frac{\Delta_{S\downarrow}-\mu}{2kT}\right). \quad (31)$$

The current $I(\mu)$ shows the standard sequential tunneling peak shape, determined by the usual cosh dependence on temperature, which is slightly modified by

$$h(T)=2W_{\uparrow\downarrow}+(2\gamma-W_{\uparrow\downarrow})f_1(\Delta_{S\downarrow}+\Delta\mu/2). \quad (32)$$

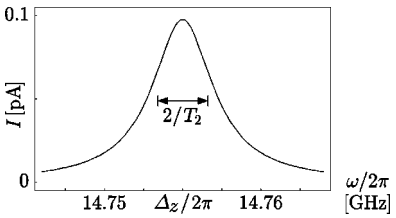

FIG. 3. The stationary current $I(\omega)$ [Eq. (30)] for $kT<\Delta\mu$, $B_z=0.5$ T, $B_x^0=0.45$ G, $T_1=1$ μs, $T_2=100$ ns, $\gamma_1=5\times10^6$ s^{-1}, and $\gamma_2=5\gamma_1$, i.e., satisfying $W_\omega^{\max}<\gamma_1<1/T_2$. Here, the linewidth gives a lower bound for the intrinsic spin decoherence time T_2 (shown schematically by the arrow), while it becomes equal to $2/T_2$ for $B_x^0=0.08$ G and $W_\omega^{\max}\ll\gamma_1=5\times10^5$ s$^{-1}\ll 2/T_2$, where $I(\omega=\Delta_z)\approx 1.5$ fA.

Most importantly, the current $I(\omega)$ of the satellite peak [Eqs. (30) and (31)] is proportional to the spin-flip rate W_ω. Thus, $I(\omega)$ or, equivalently, $I(B_z)$ has a Lorentzian shape with resonance peak at $\omega=\Delta_z$ of width $2V_{\downarrow\uparrow}$. Since $V_{\downarrow\uparrow}\geqslant 1/T_2$, this width provides a lower bound on the *intrinsic* spin decoherence time T_2 of a single dot spin. For weak tunneling $\gamma_1<2/T_2$, this bound saturates; i.e., the width $2V_{\downarrow\uparrow}$ becomes $2/T_2$. Note that the current also shows resonant behavior for $\Delta\mu=0$ and $\gamma_l^{\uparrow}\neq\gamma_l^{\downarrow}$ [Eq. (A2)]; i.e., a lower bound for T_2 can also be measured via a current due to pumping.

We point out the similarity of our proposal to ESR spectroscopy,[19] where absorption or emission linewidths of the ESR field provide information on decoherence. In contrast to these techniques, we are considering here linewidths in resonance of the current, which allows us to access even single spins, since very low currents can be measured accurately.

For Eqs. (30) and (31) we have assumed that W_ω is small compared to the tunneling or the spin relaxation rates. Therefore, we have neglected the contributions of W_ω in the denominator of these expressions. To take these contributions into account, we note that $W_\omega/(\alpha+W_\omega)$ as a function of ω is still a Lorentzian, but with an increased width $w=2V_{\downarrow\uparrow}\sqrt{1+W_\omega^{\max}/\alpha}$. Therefore, the current $I(\omega)$ has the linewidth

$$w=2V_{\downarrow\uparrow}\sqrt{1+\frac{W_\omega^{\max}(3\gamma_1+4\gamma_2)}{\gamma_1(\gamma_1+\gamma_2)+W_{\uparrow\downarrow}(\gamma_1+2\gamma_2)}}, \quad (33)$$

for $kT<\Delta\mu$ [Eq. (30)], and

$$w=2V_{\downarrow\uparrow}\sqrt{1+W_\omega^{\max}[4-f_1(\Delta_{S\downarrow}+\Delta\mu/2)]/h(T)}, \quad (34)$$

for $kT>\Delta\mu$ [Eq. (31)]. Since the linewidth is increased by this correction, the inverse linewidth is still a lower bound for T_2.

C. Universal conductance ratio

For increasing W_ω, the satellite peak in the current $I(\mu)$ increases while the main peak decreases, as shown in Fig. 2(b). Further, as function of kT, the peak is slightly shifted. Explicitly, for $\gamma_l^{\uparrow}=\gamma_l^{\downarrow}$ and $\Delta_z>\Delta\mu$, kT, we find from Eq. (29) the position of the satellite peak:

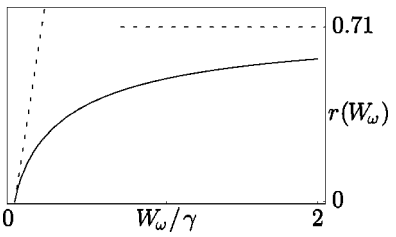

FIG. 4. The current ratio r of the main and the satellite peak as a function of the effective spin-flip rate W_ω [Eq. (37)]. The dashed line shows the saturation of r for $W_\omega\gg\gamma$ at the universal conductance ratio $r_0\approx 0.71$ [Eq. (38)].

$$\mu_{\rm ESR}=\Delta_{S\downarrow}-\frac{kT}{2}\ln\left\{\frac{W_{\uparrow\downarrow}/2+W_{\downarrow\uparrow}+3W_\omega/2+\gamma}{W_{\uparrow\downarrow}+W_{\downarrow\uparrow}+2W_\omega}\right\}. \quad (35)$$

The position of the main peak is

$$\mu_0=\Delta_{S\uparrow}+\frac{kT}{2}\ln\left\{\frac{W_{\uparrow\downarrow}+2W_{\downarrow\uparrow}+3W_\omega+2\gamma}{W_{\uparrow\downarrow}+W_{\downarrow\uparrow}+2W_\omega+2\gamma}\right\}. \quad (36)$$

An experimentally accessible quantity is the ratio of the two current peaks or, equivalently (for linear response $\Delta\mu<kT$), the ratio of the conductances $r(W_\omega)=I(\mu_{\rm ESR})/I(\mu_0)=G(\mu_{\rm ESR})/G(\mu_0)$. For this, we evaluate the stationary current at the gate voltages defined by Eqs. (35) and (36), and find, for $\Delta\mu<kT$ and $W_{\uparrow\downarrow}<W_\omega$,

$$r(W_\omega)=\frac{2W_\omega\left(1+\sqrt{1+\dfrac{W_\omega}{2W_\omega+2\gamma}}\right)^2}{4\sqrt{W_\omega}\sqrt{3W_\omega+2\gamma}+(7W_\omega+2\gamma)}; \quad (37)$$

see Fig. 4. On the one hand, for small spin-flip rates, $W_\omega<\gamma$, the ratio r is $4W_\omega/\gamma$; i.e., at ESR resonance, $r(B_x^0)=(g\mu_B B_x^0)^2/(2V_{\downarrow\uparrow}\gamma)$. If the tunneling rates and field strengths are known, this provides a further method for measuring a lower bound of the single-spin decoherence time. On the other hand, this peak ratio [Eq. (37)] can be used to measure the ratio W_ω/γ, useful for estimating the additional peak broadening due to other limiting processes, as discussed in Sec. III B; cf. Eqs. (33) and (34). It is noteworthy that the ratio r saturates for $W_\omega\gg\gamma$ at the *universal conductance ratio*

$$r_0=\frac{5+2\sqrt{6}}{7+4\sqrt{3}}\approx 0.71. \quad (38)$$

For a larger bias, but still $\Delta\mu<\Delta_z$, and for $W_\omega\gg\gamma$, the ratio becomes

$$r_0\left(\frac{\Delta\mu}{kT}\right)=\frac{(\sqrt{3}+\sqrt{2}e^{\Delta\mu/2kT})^2\gamma_1+(\sqrt{2}+\sqrt{3}e^{\Delta\mu/2kT})^2\gamma_2}{(2+\sqrt{3}e^{\Delta\mu/2kT})^2\gamma_1+(\sqrt{3}+2e^{\Delta\mu/2kT})^2\gamma_2}. \quad (39)$$

For $\gamma_1=\gamma_2$, the numerical value of r_0 remains 0.71 for all values $\Delta\mu$. Generally, r_0 is between 2/3 (for $\gamma_1\gg\gamma_2$) and 3/4 (for $\gamma_1\ll\gamma_2$), where r_0 takes these extremal values for $\Delta\mu>kT$.

Note that the current at the satellite peak is never larger than at the main peak. This asymmetry is best explained in the limit $\Delta\mu>kT$, when the ratio becomes $r_0(\infty)=(2\gamma_1+3\gamma_2)/(3\gamma_1+4\gamma_2)$. Since $W_\omega>\gamma$, the Rabi spin flips

equilibrate the populations $\rho_\uparrow$ and $\rho_\downarrow$. Thus, the stationary populations of the states are $\rho_S=\eta W_{\rm in}$, and $\rho_\uparrow=\rho_\downarrow=\eta W_{\rm out}$, where $\eta=1/(W_{\rm in}+2W_{\rm out})$ is a normalization factor, $\eta_{\rm ESR}$ at the satellite peak, and η_0 at the main peak. The rates $W_{\rm in(out)}$ include all processes of electrons tunneling into (out of) the dot. Note that at the satellite peak $\mu=\mu_{\rm ESR}$, a spin-up electron tunneling from lead 1 is the only process where an electron tunnels onto the dot, i.e., $W_{\rm in}(\mu_{\rm ESR})=\gamma_1$, whereas at the main peak $\mu=\mu_0$, the only tunnel process out of the dot is an electron with spin down into the right lead, i.e., $W_{\rm out}(\mu_0)=\gamma_2$. At the satellite peak, both spin-up and -down electrons can tunnel from the dot to lead 2; thus, the current is given by $I(\mu_{\rm ESR})=2\gamma_2\rho_S=2\gamma_1\gamma_2\eta_{\rm ESR}$, with $\eta_{\rm ESR}=1/(3\gamma_1+4\gamma_2)$. At the main peak, electrons can tunnel from lead 1 onto the dot, and the current is $I(\mu_0)=\gamma_1(\rho_\uparrow+\rho_\downarrow)=2\gamma_1\gamma_2\eta_0$, with $\eta_0=1/(2\gamma_1+3\gamma_2)$. Thus, the conductance ratio is given as $r_0=\eta_{\rm ESR}/\eta_0$, and we immediately obtain $r_0(\infty)$ in accordance with Eq. (39). Therefore, the reason for $r_0<1$ is that at the satellite peak three out of four tunnel processes contribute to $W_{\rm out}$, and thus $\eta_{\rm ESR}<\eta_0$, while only one contributes at the main peak.

IV. EVEN-TO-ODD SEQUENTIAL TUNNELING

Up to now we have considered sequential tunneling currents with odd-to-even transitions of the number of electrons on the dot. Now we consider a different filling on the dot, with even-to-odd transitions. The state with N even is $|\bar{S}\rangle$ (involving different orbital states as for $|S\rangle$), and the states with $N+1$ are $|\uparrow\rangle$ and $|\downarrow\rangle$. This system can be described with the same formalism as before, but with the tunneling rates $W_{\bar{S}\downarrow}=\Sigma_l W^l_{\bar{S}\downarrow}$, $W_{\downarrow\bar{S}}=\Sigma_l W^l_{\downarrow\bar{S}}$,

$$W^l_{\bar{S}\downarrow}=\gamma^\downarrow_l[1-f_l(\Delta_{\downarrow\bar{S}})],\quad W^l_{\downarrow\bar{S}}=\gamma^\downarrow_l f_l(\Delta_{\downarrow\bar{S}}),\qquad (40)$$

and with $W_{\bar{S}\uparrow}$, $W_{\uparrow\bar{S}}$, $W^l_{\bar{S}\uparrow}$, and $W^l_{\uparrow\bar{S}}$ defined analogously. The master equation of this system is given by Eqs. (16)–(21) upon replacing the subscripts S by $\bar{S}$. Since $W_{\downarrow\bar{S}}$ describes an electron tunneling onto the dot, whereas $W_{\downarrow S}$ describes an electron tunneling out of the dot, the stationary current through the dot is given by Eq. (22) after changing its sign and replacing the subscripts, resulting in

$$I_2=-e(W^2_{\uparrow\bar{S}}+W^2_{\downarrow\bar{S}})\rho_{\bar{S}}+eW^2_{\bar{S}\uparrow}\rho_\uparrow+eW^2_{\bar{S}\downarrow}\rho_\downarrow.\qquad (41)$$

By comparing Eqs. (11) and (12) with Eq. (40) and Eq. (22) with Eq. (41), we find that the formulas for the current are modified by the replacements $f_l(\Delta_{S\downarrow})\to[1-f_l(\Delta_{\downarrow\bar{S}})]$, $\gamma^\uparrow_l\to\gamma^\downarrow_l$, $I^\uparrow_l\to-I^\downarrow_l$, and analogously for opposite spins. For completeness, we give in the Appendix the formula for the stationary current $I^\downarrow_2$ [Eq. (A3)], which is obtained by applying the above replacements to Eq. (A1). In Sec. III B we have identified the regime of the spin satellite peak, which can be used to measure the decoherence time T_2. For the setup considered here, an analogous regime is $\mu_1>\Delta_{\downarrow\bar{S}}>\mu_2>\Delta_{\uparrow\bar{S}}$; see Fig. 5(a). The current at the spin satellite peak is then given by Eqs. (30) and (31) in the corresponding regimes, after interchanging γ_1 with γ_2, replacing $f_1\to(1-f_1)$ and $\Delta_{S\downarrow}\to\Delta_{\downarrow\bar{S}}$.

For antiferromagnetic filling of the dot, one can use particle-hole symmetry to show that the two cases, odd-to-even and even-to-odd transitions, are equivalent. Indeed, the tunneling from, say, a spin $\uparrow$ electron from the dot into the lead, $|\uparrow\rangle\to|\bar{S}\rangle$, can be regarded as a spin $\uparrow$ hole which tunnels from the lead onto the dot, which was initially occupied by a spin $\downarrow$ hole and now forms a hole singlet, i.e., $|\downarrow_h\rangle\to|S_h\rangle$. With this picture in mind, above modifications become obvious.

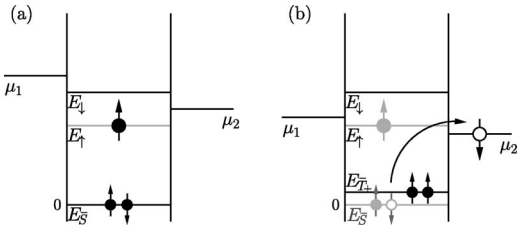

FIG. 5. (a) Setup for measuring T_2, with $\mu_1>E_\downarrow>\mu_2$ (for $E_{\bar{S}}=0$). A lower-lying state occupied by a singlet (corresponding to state $|\bar{S}\rangle$) illustrates the antiferromagnetic filling of the dot. (b) Dot which should act as spin filter, allowing only spin $\uparrow$ to pass. However, in the setup (b), the singlet-triplet spacing $E_{T_+}-E_{\bar{S}}$ is too small compared to $\Delta\mu=\mu_1-\mu_2$. Here, if the initial dot state is $|\uparrow\rangle$ (shown in gray), an electron with spin $\downarrow$ from a lower-lying state can tunnel onto the right dot, leaving a triplet on the dot (black), thus the spin filter does not operate properly. This problem disappears if the number of electrons on the dot can be reduced down to zero.

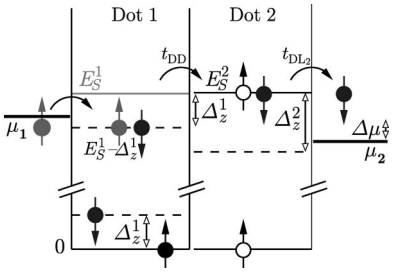

FIG. 6. Spin-inverter setup, where the ESR field generates spin flips on dot 1 and the (additional) dot 2 acts as a spin filter, allowing only spin-$\downarrow$ electrons to tunnel into lead 2. We consider the regime $|t_{\rm DD}|<|t_{\rm DL_2}|$, $E^1_S\approx E^2_S$, $\Delta^1_z\neq\Delta^2_z$, and $E^i_S>\mu_i>E^i_S-\Delta^i_z$, for $i=1,2$. The allowed transition sequence is schematically given by $\uparrow\textcircled{\uparrow}_1\textcircled{\uparrow}_2\overset{\rm ESR}{\to}\uparrow\textcircled{\downarrow}_1\textcircled{\uparrow}_2\to\textcircled{\uparrow\downarrow}_1\textcircled{\uparrow}_2\to\textcircled{\uparrow}_1\textcircled{\uparrow\downarrow}_2\leftrightarrow\textcircled{\uparrow}_1\textcircled{\uparrow}_2\downarrow$ (see text), where "$\leftrightarrow$" means a coherent tunneling process.

V. SPIN INVERTER

In this section we describe a setup with which spin-dependent tunneling $\gamma^\downarrow_l\neq\gamma^\uparrow_l$ can be achieved. Alternatively, spin-polarized leads (see Sec. VIII for details) or spin-dependent tunneling barriers could be used. This setup, shown in Fig. 6, consist of two dots, "dot 1" and "dot 2," which are coupled in series with interdot tunneling amplitude $t_{\rm DD}$. Dot 2 acts as a spin filter[24] and is coupled to the lead 2 with tunneling amplitude $t_{\rm DL_2}$. We write the Zeeman splitting Δ^d_z, the energy E^d_n of state $|n\rangle$, and the chemical potential

$\Delta^d_{S\sigma}$ with an index for dot $d=1,2$. We assume that dot 2 remains unaffected by the ESR field, which can be achieved, e.g., by applying B_x and/or B_z locally or with different g factors for dot 1 and dot 2. This assumption is taken into account by choosing $\Delta^1_z \neq \Delta^2_z$.

A. Spin filter

We briefly review the concept of using a quantum dot as spin filter,[24] as it is important for the description of the spin inverter. If the dot is initially in state $|\uparrow\rangle$, only a spin $\downarrow$ electron can tunnel onto the dot, forming a singlet. Most importantly, the Zeeman splitting in the dot should be such that $\Delta_z > \Delta_{S\downarrow} - \mu_2$. This ensures proper operation of the spin filter: because of energy conservation, only the electron with spin $\downarrow$ can tunnel from the dot to the lead, leaving the dot always in state $|\uparrow\rangle$ after an electron has passed. Therefore, the sequential tunneling current is spin $\downarrow$ polarized. There is a small spin-$\uparrow$ cotunneling current, however, which is suppressed by a factor[24] $\gamma \max\{kT,\Delta\mu\}/(E_{T_+}-E_S)^2$. Note that for efficient spin filtering, it is favorable to have the singlet state $|S\rangle$ as ground state with an even number of electrons on the dot, since the denominator of the suppression factor can become large, i.e., $E_{T_+}-E_S > \Delta_z$. Otherwise, if the triplet state $|T_+\rangle = |\uparrow\uparrow\rangle$ is the ground state, only spin-$\uparrow$ sequential tunneling current can flow through the dot. However, the spin-$\downarrow$ cotunneling current involves the triplet state $|T_0\rangle = (|\uparrow\downarrow\rangle + |\downarrow\uparrow\rangle)/\sqrt{2}$, and the suppression factor is given by $\gamma \max\{kT,\Delta\mu\}/(\Delta_z)^2$; i.e., the cotunneling current is not suppressed efficiently.[39]

B. Implementation of the spin inverter

For implementation of the spin inverter, the Zeeman splitting in dot 2 should be such that $\Delta^2_z > \Delta^1_{S\downarrow} - \mu_2$, ensuring that dot 2 acts as a spin filter. The coupling of dot 2 to the lead shall be strong such that electrons escape rapidly from dot 2 into lead 2. This leads to resonant tunneling with resonance width $\Gamma_2 = 2\pi\nu_\downarrow |t_{\mathrm{DL}_2}|^2$. We require $\Gamma_2 < \Delta^2_{S\uparrow} - \mu_2$, i.e., that the broadened level of dot 2 be above μ_2. This excludes contributions from electrons tunneling from lead 2 onto dot 2, as shown in Ref. 40.

We calculate the rates $\hat{\gamma}^\uparrow$ and $\hat{\gamma}^\downarrow$ for tunneling from dot 1 via dot 2 into lead 2 in a T-matrix approach.[41,40] We use the tunnel Hamiltonian $H_T = H_{\mathrm{DD}} + H_{\mathrm{DL}_2}$, where H_{DD} describes tunneling from dot 1 to dot 2 and H_{DL_2} from dot 2 to lead 2. The transition rates are $W_{fi} = 2\pi |\langle f|T(\varepsilon_i)|i\rangle|^2 \delta(\varepsilon_f - \varepsilon_i)$, where lead 2 is initially at equilibrium and with the T matrix

$$T(\varepsilon_i) = \lim_{\eta \to +0} H_T \sum_{n=0}^{\infty} \left(\frac{1}{\varepsilon_i + i\eta - H_{\mathrm{dot}} - H_{\mathrm{lead}}} H_T \right)^n . \quad (42)$$

We take the leading order in H_{DD} and sum up the contributions from all orders in H_{DL_2}. We then integrate over the final states in lead 2 and obtain the Breit-Wigner transition rate of an electron with spin $\downarrow$ to tunnel from dot 1 to lead 2 via the resonant level E^2_S of dot 2,

$$\hat{\gamma}^\downarrow = \frac{|t_{\mathrm{DD}}|^2 \Gamma_2}{(\Delta^1_{S\uparrow} - \Delta^2_{S\uparrow})^2 + (\Gamma_2/2)^2} . \quad (43)$$

In the spin filter regime considered here, dot 2 is always in state $|\uparrow\rangle$. Thus, tunneling of an electron with spin $\uparrow$ would involve the triplet level E_{T_+} on dot 2, which is out of resonance, and thus $\hat{\gamma}^\uparrow$ is suppressed to zero (up to cotunneling contributions, see Sec. II F). The state of dot 1 and the current through the setup is again described by the master equation [Eqs. (16)–(21)] with the tunneling rates $W^2_{S\downarrow} = W^2_{\downarrow S} = W^2_{S\uparrow} = 0$ and $W^2_{\uparrow S} = \hat{\gamma}^\downarrow$. Thus, we can use all previous results for one dot in Sec. III A, but with $\gamma^\downarrow_2 \to \hat{\gamma}^\downarrow$, $\gamma^\uparrow_2 \to 0$, and $f_2(\Delta_{S\uparrow}) = 0$. Note that even for zero bias $\Delta\mu = 0$, a pumping current flows from lead 1 via the dots 1 and 2 to lead 2; see Eq. (A2) and the Appendix.[42] We point out that this setup (see Fig. 6) acts as a *spin inverter*; i.e., only spin-$\uparrow$ electrons are taken as input (lead 1), while the output (lead 2) consists of spin-$\downarrow$ electrons. In particular, the spin inverter does not require a change in the direction of the external magnetic field.[25]

VI. ROTATING ESR FIELDS

It is interesting to study *rotating* magnetic fields in addition to linearly oscillating fields as studied above. With rotating fields, it is possible to calculate the time evolution of the density matrix of the dot exactly. In particular, the stationary solution of the master equation is obtained in a controlled approach and no rotating wave approximation is necessary. However, rotating fields are experimentally more difficult to produce than linearly oscillating fields.

We consider a clockwise rotating field with amplitude $B^0_\perp$, described by

$$H_{\mathrm{ESR}} = -\frac{1}{4}\Delta_\perp [\sigma_x \cos(\omega t) - \sigma_y \sin(\omega t)], \quad (44)$$

where $\Delta_\perp = 2g\mu_{\mathrm{B}} B^0_\perp$. Thus, for $\Delta_x = \Delta_\perp$ we have chosen the amplitude of the rotating field to be only half the amplitude of the linearly oscillating field, since both lead to the same effective spin-flip rate W_ω. Using Eq. (5) we immediately obtain the master equation, which is given by Eqs. (16)–(21) after the following replacements. The last terms in Eqs. (16) and (17) become $\mp(\Delta_\perp/2)\ \mathrm{Im}[e^{i\omega t}\rho_{\downarrow\uparrow}]$, respectively. Equation (19) is replaced by

$$\dot{\rho}_{\downarrow\uparrow} = -i\Delta_z \rho_{\downarrow\uparrow} + i\frac{\Delta_\perp}{4} e^{-i\omega t}(\rho_\uparrow - \rho_\downarrow) - V_{\downarrow\uparrow}\rho_{\downarrow\uparrow} . \quad (45)$$

We transform to the rotating frame $|\uparrow\rangle_r = e^{i\omega t/2}|\uparrow\rangle$ and $|\downarrow\rangle_r = e^{-i\omega t/2}|\downarrow\rangle$ such that $\rho_{\downarrow\uparrow} = e^{-i\omega t}\rho^r_{\downarrow\uparrow}$. This transformation removes the time dependence of the coefficients in the master equation, which we shall now write as $\dot{\boldsymbol{\rho}}^r_{\mathrm{D}} = \mathcal{M}\boldsymbol{\rho}^r_{\mathrm{D}}$. The equations for $\dot{\rho}^r_{S\uparrow}$ and $\dot{\rho}^r_{S\downarrow}$ decouple and we write the remaining part of the superoperator $\mathcal{M}$ as matrix in the basis $\{\rho^r_\uparrow, \rho^r_\downarrow, \rho^r_S, \mathrm{Re}[\rho^r_{\downarrow\uparrow}], \mathrm{Im}[\rho^r_{\downarrow\uparrow}]\}$,

$$\mathcal{M}=\begin{pmatrix} -(W_{\downarrow\uparrow}+W_{S\uparrow}) & W_{\uparrow\downarrow} & W_{\uparrow S} & 0 & -\Delta_\perp/2 \\ W_{\downarrow\uparrow} & -(W_{\uparrow\downarrow}+W_{S\downarrow}) & W_{\downarrow S} & 0 & \Delta_\perp/2 \\ W_{S\uparrow} & W_{S\downarrow} & -(W_{\uparrow S}+W_{\downarrow S}) & 0 & 0 \\ 0 & 0 & 0 & -V_{\downarrow\uparrow} & (\Delta_z-\omega) \\ \Delta_\perp/4 & -\Delta_\perp/4 & 0 & -(\Delta_z-\omega) & -V_{\downarrow\uparrow} \end{pmatrix}. \tag{46}$$

The master equation can now be solved exactly by calculating the eigenvalues λ_i of $\mathcal{M}$. Since the total probability is conserved, $\Sigma_n \dot{\rho}_n = 0 = \Sigma_{nm}\mathcal{M}_{nm}\rho_m$, where n is summed over the diagonal elements and m over diagonal and off-diagonal elements of $\boldsymbol{\rho}_{\mathrm{D}}$. By considering linearly independent initial conditions for $\boldsymbol{\rho}_{\mathrm{D}}$, we see that $\Sigma_n \mathcal{M}_{nm}=0$, for every m. Thus, adding up the rows in $\mathcal{M}$ for the diagonal elements of $\boldsymbol{\rho}_{\mathrm{D}}$ gives zero, which is satisfied explicitly by adding the first three rows in Eq. (46). Therefore, $\mathcal{M}$ does not have full row rank and there is an eigenvalue $\lambda_0=0$ with eigenspace describing the stationary solution. The eigenvalues of $\mathcal{M}$ are

$$\left\{0, -V_{\downarrow\uparrow}, -3W, -\frac{1}{2}(\Sigma_W+V_{\downarrow\uparrow}\pm\sqrt{(\Sigma_W-V_{\downarrow\uparrow})^2-\Delta_\perp^2})\right\}, \tag{47}$$

with $\Sigma_W = W+W_{\uparrow\downarrow}+W_{\downarrow\uparrow}$ and where we have considered $W=W_{S\uparrow}=W_{S\downarrow}=W_{\uparrow S}=W_{\downarrow S}$ and resonance $\Delta_z=\omega$ for simplicity. If all λ_i are different, the time evolution of the density matrix is $\boldsymbol{\rho}_{\mathrm{D}}(t)=\Sigma_i c_i e^{\lambda_i t}\boldsymbol{\rho}_i$.[43] The decay of the contribution of the eigenvectors $\boldsymbol{\rho}_i$ is exponential and generally all decay rates λ_i are involved. Further, we see from the last two eigenvalues in Eq. (47) that the decay rates of $\boldsymbol{\rho}_{\mathrm{D}}$ may be a nontrivial function of the rates involved in the master equation. This should be kept in mind when one uses time-dependent ensemble properties, i.e., $\boldsymbol{\rho}_{\mathrm{D}}(t)$, to measure intrinsic rates, e.g., T_1 and T_2. We point out that the presence of very small decay rates does not necessarily prevent a decay of the initial conditions. If, say, the tunneling rates are smaller than the spin relaxation rate, $W \ll W_{\uparrow\downarrow}$, it would be interesting to study a density matrix which is described as a linear combination of the eigenvector with eigenvalue $-3W$ [Eq. (47)] and the stationary solution $\boldsymbol{\rho}_0$, i.e., $\boldsymbol{\rho}_{\mathrm{D}}(t) = \boldsymbol{\rho}_0 + ce^{-3Wt}\boldsymbol{\rho}_{3W}$, where the decay rate $3W$ is independent of $W_{\uparrow\downarrow}$. However, such an initial condition always contains contributions from state $|S\rangle$ such that, in particular, it is not possible to construct an initial spin-$\frac{1}{2}$ state which would decay only with the slow rate $3W$.

The (exact) stationary solution of the master equation can be readily obtained from Eq. (46). By eliminating $\rho^r_{\downarrow\uparrow}$ from the coupled equations, we obtain the effective spin-flip rate

$$W_\omega = \frac{\Delta_\perp^2}{8}\frac{V_{\downarrow\uparrow}}{(\omega-\Delta_z)^2+V_{\downarrow\uparrow}^2}, \tag{48}$$

which is equivalent to Eq. (25). Thus, all the results for the stationary currents from Sec. III apply and are exact for the case of rotating magnetic fields.

VII. COTUNNELING

We now consider the cotunneling regime[44–46] $\Delta_{S\uparrow}$, $\Delta_{S\downarrow} > \mu_1$, $\mu_2 \gg E_\downarrow$, $E_\uparrow$, where the number of electrons on the dot is odd; thus the state on the dot is described by $|\uparrow\rangle$ and $|\downarrow\rangle$. The leading-order tunnel processes is now the tunneling of electrons from lead l onto the dot, forming a virtual state $|n\rangle$, followed by tunneling into lead l'. The spin state on the dot changes $\sigma\to\sigma'$. This process is called elastic cotunneling for $\sigma=\sigma'$ and inelastic cotunneling for $\sigma\neq\sigma'$. Note that in the absence of an ESR field, the dot relaxes into its spin ground state and no inelastic cotunneling processes, exciting the dot spin, occur for $\Delta\mu<\Delta_z$. However, if an ESR field is present, the dot spin can be excited by spin flips. Then, inelastic cotunneling processes, which relax the dot spin, can occur. These processes either contribute to transport or produce a particle-hole excitation in lead 1 or 2 [see Figs. 7(b) and 7(c)].

These cotunneling rates are calculated in a ''golden rule'' approach,[24] which is known to be consistent with a microscopic derivation,[46]

$$W^{l'l}_{\sigma'\sigma} = 2\pi\nu^2\int d\epsilon f_l(\epsilon)[1-f'_l(\epsilon-\Delta_{\sigma'\sigma})]\left|\sum_n \frac{t_{l'\sigma'n}t^*_{l\sigma n}}{\Delta_{n\sigma}-\epsilon}\right|^2, \tag{49}$$

where the possible spin dependence of ν has been absorbed into t, $\Delta_{\sigma'\sigma}=E_{\sigma'}-E_\sigma$ is the change of Zeeman energy on the dot, and $\Delta_{n\sigma}=E_n-E_\sigma$ is the energy cost of the virtual intermediate state. Here, $t_{l\sigma n}$ are the tunneling amplitudes, where $t_{l\downarrow S}=t_l^\uparrow$ has already been introduced in Eq. (13). The cotunneling current through the dot can be calculated by summing up the contributing tunneling rates, as we have done for Eq. (22),

$$I_{\mathrm{CT}} = e\sum_{\sigma\sigma'}(W^{21}_{\sigma'\sigma}-W^{12}_{\sigma'\sigma})\rho_\sigma. \tag{50}$$

We point out that by treating the cotunneling processes with golden rule rates, only classically allowed dot states are considered. Thus, the number of charges on the dot is fixed and no charge can temporarily accumulate as for sequential tunneling. In particular, we have neglected quantum charge fluctuations on the dot. Therefore, within our master equation approach for cotunneling, the charge currents in both leads are equal, $I_1(t)=I_2(t)$. This equality is valid for ''coarse-grained'' expectation values of the current (and other physical observables). In this approximation, one smoothens out the quantum fluctuations by averaging over the short-time behavior; i.e., one considers only the behavior on time scales

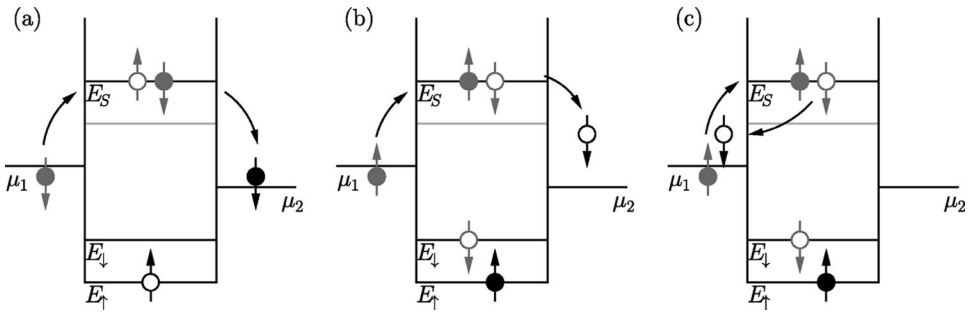

FIG. 7. Cotunneling processes involving $|S\rangle$ for $\Delta_z > \Delta\mu$. (a) Elastic cotunneling. The cotunneling sequence $\downarrow(\uparrow) \to (\uparrow\downarrow) \to (\uparrow)\downarrow$, involving the virtual state $|S\rangle$ on the dot with virtual energy cost $\Delta_{S\uparrow} - \mu_1$. An equivalent process is possible when the initial and final dot state is $|\downarrow\rangle$, however with a virtual energy cost reduced by Δ_z. These elastic cotunneling processes contribute to transport and to spin decoherence, while they do not contribute to spin relaxation (i.e., T_1). (b) Inelastic cotunneling from lead 1 into lead 2 via the sequence $\uparrow(\downarrow) \to (\uparrow\downarrow) \to (\uparrow)\downarrow$. Note that tunneling of an electron from lead 2 into lead 1 is also possible, since the energy gain Δ_z from the dot relaxation is larger than the bias $\Delta\mu$. (c) Inelastic cotunneling, where only one lead is involved. The process shown here leads to a particle-hole excitation in lead 1. While it does not directly contribute to transport, it contributes to spin relaxation and spin decoherence of the dot.

larger than the lifetime $1/(\Delta_{S\sigma} - \mu)$ of the virtual states on the dot. However, when the charge imbalance due to the virtual states is taken into account in a microscopic treatment, one can find pronounced peaks in the noise $S(\omega)$ for $|\omega|$ corresponding to the virtual energy cost, as was shown in Ref. 47.

The inelastic cotunneling provides spin relaxation processes in addition to those contributing to T_1, totaling in $W^{\mathrm{CT}}_{\uparrow\downarrow} = W_{\uparrow\downarrow} + \Sigma_{ll'} W^{l'l}_{\uparrow\downarrow}$. For processes with $l' = l$, particle-hole excitations are produced in lead l. We are interested in the regime $\Delta\mu < \Delta_z$, where (inelastic) cotunneling does not excite the dot spin, i.e., $W^{\mathrm{CT}}_{\downarrow\uparrow} = W_{\downarrow\uparrow}$. In analogy to Eq. (15), we take a phenomenological total spin decoherence rate

$$V^{\mathrm{CT}}_{\downarrow\uparrow} = \frac{1}{T_2} + \frac{1}{2} \sum_{ll'\sigma\sigma'} W^{l'l}_{\sigma'\sigma}, \tag{51}$$

where all spin relaxation and tunneling processes are taken into account. The master equation for the dot in the cotunneling regime and in the presence of a linearly polarized ESR field becomes

$$\dot{\rho}_\uparrow = -W^{\mathrm{CT}}_{\downarrow\uparrow}\rho_\uparrow + W^{\mathrm{CT}}_{\uparrow\downarrow}\rho_\downarrow - \Delta_x \cos(\omega t)\ \mathrm{Im}[\rho_{\downarrow\uparrow}], \tag{52}$$

$$\dot{\rho}_\downarrow = W^{\mathrm{CT}}_{\downarrow\uparrow}\rho_\uparrow - W^{\mathrm{CT}}_{\uparrow\downarrow}\rho_\downarrow + \Delta_x \cos(\omega t)\ \mathrm{Im}[\rho_{\downarrow\uparrow}], \tag{53}$$

$$\dot{\rho}_{\downarrow\uparrow} = -i\Delta_z \rho_{\downarrow\uparrow} + i\frac{\Delta_x}{2}\cos(\omega t)(\rho_\uparrow - \rho_\downarrow) - V^{\mathrm{CT}}_{\downarrow\uparrow}\rho_{\downarrow\uparrow}. \tag{54}$$

Note that away from the sequential tunneling regime, the master equation becomes much simpler while the formulas for the rates are more involved.

For the time-averaged current we evaluate the stationary solution of the master equation in the rotating wave approximation (see Sec. III) for linearly or exactly (see Sec. VI) for circularly polarized ESR fields. This yields an effective spin-flip rate W_ω [Eqs. (25) and (48), respectively] and eliminates Eq. (54). We obtain

$$\rho_\downarrow = \frac{W_\omega + W_{\downarrow\uparrow}}{2W_\omega + W_{\downarrow\uparrow} + W_{\uparrow\downarrow} + \sum_{ll'} W^{l'l}_{\uparrow\downarrow}} \tag{55}$$

and $\rho_\uparrow = 1 - \rho_\downarrow$. We consider the case close to a sequential tunneling resonance (but still in the cotunneling regime), $\Delta_{S\sigma} - \mu_l < E_{T_+} - E_S$, such that the virtual energy cost of an intermediate triplet state is much higher than that for a singlet state. Since $(E_{T_+} - E_\sigma - \mu)/(E_S - E_\sigma - \mu) < 1$, with $\mu = (\mu_1 + \mu_2)/2$, we have to consider only cotunneling processes involving state $|S\rangle$ in Eq. (49). For $\Delta\mu$, $kT < \Delta_{S\sigma} - \mu < E_{T_+} - E_S$, the relevant elastic rates are

$$W^{21}_{\sigma\sigma} = \frac{\gamma_1\gamma_2}{2\pi}\frac{\Delta\mu}{(\Delta_{S\sigma} - \mu)^2}. \tag{56}$$

The inelastic rates are, for lead indices l, $l' = 1, 2$,

$$W^{l'l}_{\uparrow\downarrow} = \frac{\gamma_1\gamma_2}{2\pi}\frac{\Delta_z + (l' - l)\Delta\mu}{(\Delta_{S\downarrow} - \mu)(\Delta_{S\downarrow} + \Delta_z - \mu)} \tag{57}$$

$$\approx \frac{\Delta_z + (l' - l)\Delta\mu}{\Delta\mu} W^{21}_{\downarrow\downarrow}, \tag{58}$$

where Eq. (58) is valid for $\Delta_z < \Delta_{S\downarrow} - \mu$. Note that for $\Delta\mu < \Delta_z$ the inelastic rates can be much larger (by a factor of $\Delta_z/\Delta\mu$) than the elastic ones, while their contribution to the current, $W^{21}_{\uparrow\downarrow} - W^{12}_{\uparrow\downarrow} = 2W^{21}_{\downarrow\downarrow}$, is of the same order as for the elastic rates.

For $W^{\max}_\omega, W_{\uparrow\downarrow} < W^{21}_{\uparrow\downarrow}$, we obtain the cotunneling current from Eqs. (50) and (55)–(57),

$$I_{\mathrm{CT}} = \frac{e}{2\pi}\frac{\Delta\mu\gamma_1\gamma_2}{(\Delta_{S\uparrow} - \mu)^2} + eW_\omega\frac{\Delta\mu}{4\Delta_z}\left[3 - \frac{\Delta_{S\downarrow} - \mu}{\Delta_{S\uparrow} - \mu} + \frac{\Delta_z}{\Delta_{S\downarrow} - \mu}\right] \tag{59}$$

$$\approx \frac{e}{2\pi}\frac{\Delta\mu\gamma_1\gamma_2}{(\Delta_{S\uparrow} - \mu)^2} + eW_\omega\frac{\Delta\mu}{2\Delta_z}. \tag{60}$$

The first term in Eq. (59) results from elastic cotunneling with spin ground state $|\uparrow\rangle$ on the dot. The second term represents the increased current if the spin is flipped into state $|\downarrow\rangle$ before cotunneling occurs, since then both elastic and

inelastic cotunneling processes contribute to the current. The current $I_{\rm CT}$ is proportional to W_ω, up to a constant background and thus shows, as a function of ω, a resonant peak at $\omega=\Delta_z$ of width $2V_{\downarrow\uparrow}$. Thus, the intrinsic spin decoherence time T_2 is accessible in the cotunneling current as well as in the sequential tunneling (see Sec. III B). Generally, the cotunneling current is much smaller than the sequential tunneling current, and thus it might seem more difficult to detect T_2 in the cotunneling regime. However, since the current and the decoherence rate due to tunneling are proportional to γ^2, the small currents can be compensated by choosing more transparent tunnel barriers, i.e., larger γ. Then, the current and the decoherence rate in the cotunneling regime can become comparable to the sequential tunneling values given in Sec. III B. For illustration we give the following estimates. For $B_z=1$ T, $B_x^0=2$ G, $g=2$, $\gamma_1=\gamma_2=5\times10^9$ s^{-1}, $T_1=1$ μs, $T_2=100$ ns, $\Delta_{S\downarrow}-\mu=\Delta_z$, and $\Delta\mu=\Delta_z/5$, the cotunneling current as a function of the ESR frequency ω is 0.17 pA away from resonance and exhibits a resonance peak of $I_{\rm CT}^{\rm max}=0.31$ pA, with half-width $V_{\downarrow\uparrow}^{\rm CT}=3.41\times10^7$ s^{-1}.

VIII. SPIN READOUT WITH SPIN-POLARIZED LEADS

An electron spin on a quantum dot can be used as a single spin memory (or as a quantum bit for quantum computation[11]) if the spin state of the quantum dot can be measured. It was shown that a quantum dot connected to fully spin-polarized leads, $\Delta_z^{\rm leads}>\varepsilon_{\rm F}>\Delta_z$, can be used for reading the spin state of the quantum dot via the charge current.[24] Such a situation can be realized with magnetic semiconductors (with effective g factors exceeding 100)[5] or in the quantum Hall regime where spin-polarized edge states are coupled to a quantum dot.[48] If the spin polarization in both leads is $\uparrow$, no electron with spin $\downarrow$ can be provided or taken by the leads (since $\nu_\downarrow=0$), and the rates $W_{S\uparrow}$ and $W_{\uparrow S}$ vanish. Thus, if the dot is initially in state $|\uparrow\rangle$, no electron can tunnel onto the dot (the formation of the triplet is forbidden by energy conservation) and $I=0$, up to negligible cotunneling contributions. However, if the dot is in state $|\downarrow\rangle$, a current can flow via the sequential tunneling transitions $\uparrow\textcircled{\downarrow}\rightarrow\textcircled{\uparrow\downarrow}\rightarrow\textcircled{\downarrow}\uparrow$. Therefore, the initial spin state of the quantum dot can be detected by measuring the current through the dot. Note that for this readout scheme, it is not necessary to have $\Delta_z>kT$ on the dot; the constraint of having spin-polarized leads is already sufficiently strong.

In the stationary regime and for $\Delta_z>kT$, the current becomes blocked due to spin relaxation ($W_{\uparrow\downarrow}$). However, this blocking can be removed by the ESR field producing spin flips on the dot (with rate W_ω). For $W_\omega<W_{\uparrow\downarrow}$, this competition leads again to a stationary current with resonant structure,

$$I(\omega)=e(W_{\downarrow\uparrow}+W_\omega)\frac{\gamma_1\gamma_2}{\gamma_2 W_{\uparrow\downarrow}+(\gamma_1+\gamma_2)W_{\downarrow\uparrow}}, \qquad (61)$$

from which $V_{\downarrow\uparrow}$ (and $1/T_2$) can be measured. Note that the relaxation rate $W_{\uparrow\downarrow}$ is rather small; thus only small ESR fields can be used, which leads to small currents.

A. Counting statistics and signal-to-noise ratio

We analyze now the time dynamics of the readout of a dot spin via spin-polarized currents. The goal is to obtain the full counting statistics and to characterize a measurement time $t_{\rm meas}$ for the spin readout. While we have considered only averaged currents so far, we now need to keep track of the number of electrons q which have accumulated in lead 2 since $t=0$.[49] The time evolution of $\rho_{\rm D}(q,t)$, now charge dependent, is described by Eqs. (16)–(21), but with replacements $W_{\downarrow S}^2\rho_S(q)\rightarrow W_{\downarrow S}^2\rho_S(q-1)$ in Eq. (17) and $W_{S\downarrow}^2\rho_\downarrow(q)\rightarrow W_{S\downarrow}^2\rho_\downarrow(q+1)$ in Eq. (18). Next, we consider the distribution function $P_i(q,t)=\Sigma_n\rho_n(q,t)$ that q charges have accumulated in lead 2 after time t when the dot was in state $|i\rangle$ at $t=0$. For a meaningful measurement of the dot spin, the spin-flip times $W_{\uparrow\downarrow}^{-1}$, $W_{\downarrow\uparrow}^{-1}$ and $1/\Delta_x$ must be smaller than $t_{\rm meas}$ and are neglected. Equations (16)–(21) then decouple except Eqs. (17) and (18), which we solve for $\rho_\uparrow=1$ and for $\rho_\downarrow=1$ at $t=0$. The general solution follows by linear combination. First, if the dot is initially in state $|\uparrow\rangle$, no charges tunnel through the dot, and thus $P_\uparrow(q,t)=\delta_{q0}$. Second, for the initial state $|\downarrow\rangle$, we consider $kT<\Delta\mu$ and equal rates $W_{S\downarrow}^1=W_{\downarrow S}^2=W$. We relabel the density matrix $\rho_\downarrow(q)\rightarrow\rho_{m=2q}$ and $\rho_S(q)\rightarrow\rho_{m=2q+1}$, and Eqs. (17) and (18) become

$$\dot{\rho}_m=W(\rho_{m-1}-\rho_m), \qquad (62)$$

with solution $\rho_m(t)=(Wt)^m e^{-Wt}/m!$ (Poissonian distribution). We obtain the counting statistics

$$P_\downarrow(q,t)=\frac{(Wt)^{2q}e^{-Wt}}{(2q)!}\left(1+\frac{Wt}{2q+1}\right). \qquad (63)$$

Experimentally, $P_\downarrow(q,t)$ can be determined by time series measurements or by using an array of independent dots (see Sec. IX A). The inverse signal-to-noise ratio is defined as the Fano factor,[50,51] which we calculate as

$$F_\downarrow(t)=\frac{\langle\delta q(t)^2\rangle}{\langle q(t)\rangle}=\frac{1}{2}+\frac{3-2e^{-2Wt}(4Wt+1)-e^{-4Wt}}{4(2Wt-1+e^{-2Wt})}, \qquad (64)$$

with $F_\downarrow$ decreasing monotonically from $F_\downarrow(0)=1$ to $F_\downarrow(t\rightarrow\infty)=\frac{1}{2}$. Note that for dot spin $|\uparrow\rangle$, only weak cotunneling occurs with Fano factor $F_\uparrow=1$.[46]

If we are interested in the current and noise for long times $t>W^{-1}$, we can follow the steps used in Ref. 52. We decouple the differential equations with respect to q by taking the inverse Fourier transform $\rho_{\rm D}(k)=\Sigma_q e^{-ikq}\rho_{\rm D}(q)$. Note that, for $k=0$, we recover the density matrix $\rho_{\rm D}=\rho_{\rm D}(k=0)$, where the accumulated charge is not taken into account. The probability $P_\downarrow(q,t)$ is then approximated by a Gaussian wave packet in q space with group velocity $I/e=W_{S\downarrow}^1W_{\downarrow S}^2/(W_{S\downarrow}^1+W_{\downarrow S}^2)$ and width $\sqrt{2F(I/e)t}$, and

$$F=\frac{(W_{S\downarrow}^1)^2+(W_{\downarrow S}^2)^2}{(W_{S\downarrow}^1+W_{\downarrow S}^2)^2} \qquad (65)$$

is the Fano factor.[52] However, within this approximation, valid for $Wt>1$, we cannot access the short-time behavior where only a few electrons have tunneled through the dot, which is of importance for the readout process considered here.

B. Measurement time

Using the counting statistics, we can now quantify the measurement efficiency. If, after time $t_{\rm meas}$, some charges $q>0$ have tunneled through the dot, the initial state of the dot was $|\downarrow\rangle$ with probability 1 [assuming that single charges can be detected via a single electron transistor (SET) (Ref. 51)]. However, if no charges were detected ($q=0$), the initial state of the spin memory was $|\uparrow\rangle$ with probability

$$1-P_{\downarrow}(0,t)=1-\frac{W^1_{S\downarrow}e^{-W^2_{\downarrow S}t}-W^2_{\downarrow S}e^{-W^1_{S\downarrow}t}}{W^1_{S\downarrow}-W^2_{\downarrow S}}, \qquad (66)$$

which reduces to $1-e^{-Wt}(1+Wt)$, for equal rates. Thus, roughly speaking, we find that $t_{\rm meas}\gtrsim 2W^{-1}$, as expected, while the Fano factor is $0.5<F_{\downarrow}\lesssim 0.72$. If, more generally, the threshold for detection is at m charges, $m\geqslant 1$, Eq. (66) is replaced by $1-\Sigma_{q=0}^{m-1}P_{\downarrow}(q,t)$.

We insert now realistic numbers to obtain an estimate of the fastest possible measurement time which can be achieved with this setup. For a fast spin readout, the tunneling rates and the current through the dot should be large, limited by the fact that the conductance of the dot should not exceed the single-channel conductance e^2/h. In the linear response regime and for a small bias $\Delta\mu/e$, the current is $I=e\gamma^{\uparrow}\Delta\mu/8kT<(\Delta\mu/e)(e^2/h)$ for $\gamma_1^{\uparrow}=\gamma_2^{\uparrow}$. Thus, the tunneling rates are limited by $\gamma^{\uparrow}<8kT/h=1.76\times 10^{11}(T/{\rm K})\ {\rm s}^{-1}$. For $W=\gamma^{\uparrow}=1.25\times 10^{10}\ {\rm s}^{-1}$ (corresponding to $kT<\Delta\mu$ and a current $I=1$ nA) and $m=1$, the spin state can be determined with more than 95% probability for a measurement time of $t_{\rm meas}=400$ ps and with more than 99.99% probability for $t_{\rm meas}=1$ ns.[53]

IX. RABI OSCILLATIONS OF A SINGLE SPIN IN THE TIME DOMAIN

A. Observing Rabi oscillations via current

The ESR field generates coherent Rabi oscillations of the dot spin, leading to oscillations in $\rho_{\rm D}(t)$. Since the time-dependent currents $I(t)$ in the leads are given by the populations $\rho_n(t)$ [Eq. (22)], current measurements give access to these Rabi oscillations. First, we consider a dot coupled to unpolarized leads in the regime of the spin satellite peak (see Fig. 1 and Sec. III A). For $kT<\Delta\mu$, the current in lead 2 is $I_2(t)=e(\gamma_2^{\uparrow}+\gamma_2^{\downarrow})\rho_S(t)$; i.e., ρ_S is directly accessible via measurement of $I_2(t)$.[54] Further, for $\gamma_1^{\uparrow}=\gamma_1^{\downarrow}$, the current in lead 1 is $I_1(t)=e\gamma_1(\rho_{\downarrow}-\rho_S)$, which gives access to $\rho_{\downarrow}(t)$, if the ratio γ_1/γ_2 is known. We calculate the oscillations of $I_{1,2}(t)$ explicitly by numerical integration of the master equation [Eqs. (16)–(19)]; see Fig. 8(b).

The measurement of $\rho_{\rm D}$ can be refined by using the spin readout setup with spin-polarized leads (Sec. VIII). For $kT<\Delta\mu$, the current is $I_1(t)=I_1^{\uparrow}(t)=e\gamma_1^{\uparrow}\rho_{\downarrow}(t)$ in lead 1 and $I_2(t)=I_2^{\uparrow}(t)=e\gamma_2^{\uparrow}\rho_S(t)$ in lead 2.[54] Thus, the time dependence of $\rho_{\downarrow}$ and ρ_S (and also of $\rho_{\uparrow}=1-\rho_{\downarrow}-\rho_S$) can be directly measured via the currents $I_{1,2}$; see Fig. 8(a).

Note that the electrons which tunnel onto the dot decohere the spin state on the dot (see Sec. II E). Thus, to observe Rabi oscillations in $I_{1,2}(t)$ experimentally, the Rabi frequency Δ_x must be larger than the coupling to the leads $W_{S\downarrow}$; otherwise, the strong decoherence (equivalent to a continuous measurement) suppresses the Rabi oscillations (Zeno effect; see Sec. IX C). Then, however, only very few electrons tunnel per Rabi oscillation period through the dot. To overcome the limitations of such a weak current signal and to obtain $I_{1,2}(t)$ experimentally, an ensemble average is required.

There are two possibilities to obtain averages: namely, using many dots or performing a time series measurement. First, many independent dots can be measured simultaneously by arranging the dots in parallel to increase the total current. For example, an array (ensemble) of dots and leads could be produced with standard techniques for defining nanostructures or self-assembled, or chemically synthesized dots could be placed within an insulating barrier between two electrodes. Second, time series measurement over a single dot can be performed. For this, the procedure of preparing the dot to the desired initial state—applying an ESR field and measuring the current—has to be repeated many times (see Sec. VIII A for counting statistics of the readout process). Then, assuming ergodicity, the current average of all these individual measurements corresponds to the ensemble-averaged value.

B. Decoherence in the time domain

In Fig. 8, we plot the numerical solution of Eqs. (16)–(21), showing the coherent oscillations of $\rho_{\rm D}$ and I_l, for (a) spin-polarized and (b) unpolarized leads. The decay of these oscillations is dominated by the spin decoherence rate $V_{\downarrow\uparrow}$. Since this decay can be measured via the current, $V_{\downarrow\uparrow}$ (and $1/T_2$) can be accessed directly in the time domain (see also Sec. X, Ref. 55 and Fig. 9).

C. Zeno effect

When the rate for electrons tunneling onto the dot, $W_{S\sigma}$, is increased, the coherent oscillations of $\rho_{\uparrow}$, $\rho_{\downarrow}$ become suppressed [see inset of Fig. 8(a)]. This suppression is caused by the increased spin decoherence rate $V_{\downarrow\uparrow}$ [Eq. (15)] and can be interpreted as a continuous strong measurement of the dot spin, performed by an increased number of charges tunneling onto the dot. This suppression of coherent oscillations is known as the Zeno effect.[56] Since it is visible in $\rho_{\rm D}$, it can be observed via the currents $I_{1,2}(t)$.

X. PULSED ESR AND RABI OSCILLATIONS

We now show that it is possible to observe the coherent Rabi oscillations of a single electron spin even without the requirement of measuring time-resolved currents. This can be achieved by applying ESR pulses of length t_p and by measuring time-averaged currents (over arbitrarily long

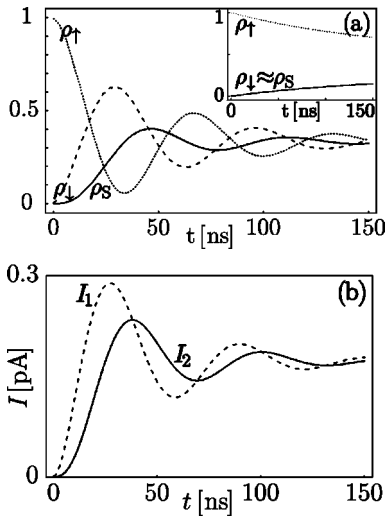

FIG. 8. Rabi oscillations of the electron spin on the dot in the time domain. We consider the regime at the spin satellite peak, $\Delta_{S\uparrow} > \mu_1 > \Delta_{S\downarrow} > \mu_2$, (see Fig. 1), and take $T_1 = 1$ μs, $T_2 = 300$ ns, $\Delta_x = 5W_{S\downarrow}$ (corresponding to $B_x^0 = 10$ G for $g = 2$), and $\rho_\uparrow = 1$ at $t = 0$. During the time span shown here, fewer than three electrons have tunneled through the dot on average. Here, the spin decoherence is dominated by the tunneling process, i.e., $W_{S\downarrow} \gg 1/T_2$. (a) Spin-polarized leads with the only nonvanishing tunnel rates $W_{S\downarrow} = W_{\downarrow S} = 4 \times 10^7$ s^{-1}. The Rabi oscillations show up in $\rho_\uparrow$ (dotted line), $\rho_\downarrow$ (dashed line), and ρ_S (solid line), which is directly visible in the current, since $I_1^\uparrow(t) \propto \rho_\downarrow$ and $I_2^\uparrow(t) \propto \rho_S$, for $kT < \Delta\mu$. In the inset, we show the case of large tunneling, $W_{S\downarrow} = W_{\downarrow S} = 10^9$ s$^{-1} \gg \Delta_x$. As a consequence of the Zeno effect (see Sec. IX C), the Rabi oscillations are suppressed. Further, $\rho_\downarrow$ and ρ_S are indistinguishable since $|\downarrow\rangle$ and $|S\rangle$ equilibrate rapidly due to the increased tunneling. (b) The time-dependent currents in unpolarized leads, $I_1(t) = e\gamma_1(\rho_\downarrow - \rho_S)$ and $I_2(t) = 2e\gamma_2\rho_S$, for $kT < \Delta\mu$, and $\gamma_l^\uparrow = \gamma_l^\downarrow = 4 \times 10^7$ s^{-1}, for $l = 1,2$.

times). Then, the time-averaged current $\overline{I}(t_p)$ as function of t_p gives access to the time evolution of the spin state on the dot for both polarized and unpolarized leads.[57] In particular, since arbitrarily long times, and thus a large number of electrons, can be used to measure $\overline{I}$, the required experimental setups are significantly simpler compared to setups which aim at measuring time-dependent currents with high resolution.

We assume a rectangular envelope for the ESR pulse with length t_p and repetition time t_r (thus $t_p < t_r$). The time when no ESR field is present, $t_r - t_p$, should be long enough such that the dot can relax into its ground state $|\uparrow\rangle$; i.e., at the beginning of the next pulse, we have $\rho_\uparrow = 1$. We calculate $\overline{I}(t_p)$ by numerical integration of the master equation [Eqs. (16)–(19)] and by subsequently averaging the (time-dependent) current [Eq. (22)] over the time interval $[0,t_r]$. The results are shown in Fig. 9(b) for unpolarized leads at the spin satellite peak (see Sec. III A) and in Fig. 9(c) for spin-polarized leads in the regime for spin readout (see Sec. VIII). In both cases, $\overline{I}(t_p)$ as a function of pulse length t_p shows the Rabi oscillations of the dot spin; i.e., the Rabi oscillations can be observed in the time domain even without time-resolved measurements.

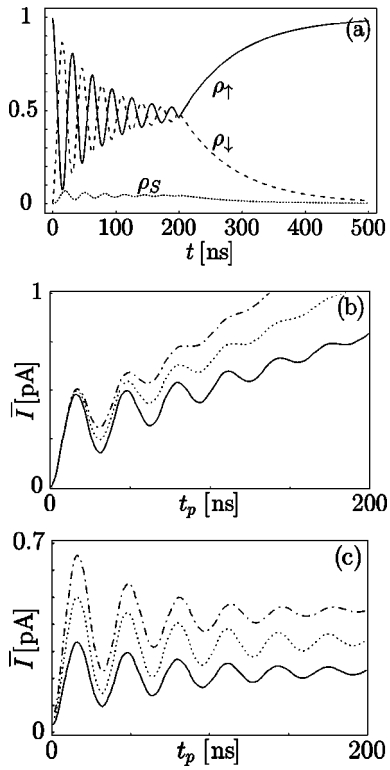

FIG. 9. Single-spin Rabi oscillations in the current $\overline{I}(t_p)$ generated by ESR pulses of length t_p. Here, $\Delta\mu > kT$, Rabi frequency $\Delta_x = 4 \times 10^8$ s^{-1} (corresponding to $g = 2$ and $B_x^0 = 20$ G), $\gamma_1 = 2 \times 10^7$ s^{-1}, $\gamma_2 = 5\gamma_1$, $T_1 = 1$ μs, and $T_2 = 150$ ns. (a) Evolution of the density matrix for unpolarized leads where a pulse of length $t_p = 200$ ns is switched on at $t = 0$, obtained by numerical integration of the master equation [Eqs. (16)–(19)]. (b) Time-averaged current $\overline{I}(t_p)$ (solid line) for unpolarized leads and a pulse repetition time $t_r = 500$ ns. We also show the current where γ_1 and γ_2 are increased by a factor of 1.5 (dotted line) and 2 (dash-dotted line). (c) Time-averaged current $\overline{I}(t_p)$ (solid line) for spin-polarized leads, $\gamma_1^\uparrow = 2 \times 10^7 \mathrm{s}^{-1}$, $\gamma_2^\uparrow = 5\gamma_1^\uparrow$, $\gamma_{1,2}^\downarrow = 0$. The pulse repetition time $t_r = 10$ μs is chosen larger than T_1. Again, we show the current for tunneling rates $\gamma_{1,2}^\uparrow$ increased by a factor of 1.5 (dotted line) and 2 (dash-dotted line). Note that in this figure $t_p < T_1$; i.e., most electrons tunnel through the dot after the pulse is switched off, thus the linear background is negligibly small.

In addition to the exact numerical evaluation of the master equation (see Fig. 9), we now give an approximate analytical expression for $\overline{I}(t_p)$. We first consider the case of unpolarized leads at the spin satellite peak (Sec. III A); for the case of spin-polarized leads, see below. For this, we need to evaluate the time average of Eq. (22). For $kT < \Delta\mu$, we get

$$\overline{I}(t_p) = e(\gamma_2^\uparrow + \gamma_2^\downarrow)\frac{1}{t_r}\int_0^{t_r} dt\,\rho_S(t). \tag{67}$$

First, we consider times t with $0 \leqslant t \leqslant t_p$, for which an ESR field is present, and ρ_D oscillates with Rabi frequency Δ_x [see Fig. 9(a) for $t \leqslant 200$ ns]. Qualitatively speaking, when $\rho_S(t)$ is integrated in Eq. (67) up to t_p, the oscillating contribution averages nearly to zero, and we obtain a back-

ground contribution $\overline{I_0}$ approximately proportional to $e(\gamma_2^{\uparrow}+\gamma_2^{\downarrow})t_p/t_r$, i.e., linear in t_p, in agreement with Fig. 9(b). For experiments, this linearity of $\overline{I_0}$ provides a first check that t_r is sufficiently long such that the dot has indeed relaxed into its ground state before the next pulse is applied. We also give an upper bound for $\overline{I_0}$ by using the inequality $\rho_S \leqslant \rho_S^{\max}=W_{S\downarrow}/(W_{S\downarrow}+W_{S\uparrow}+W_{\uparrow S})$. This is seen as follows. For $\rho_S(t)>\rho_S^{\max}$, we would have $\dot{\rho}_S(t)<0$, and thus $\rho_S(t')>\rho_S^{\max}$, for all $0\leqslant t'\leqslant t$, which would be in contradiction to the initial condition $\rho_S(0)=0$, hence indeed $\rho_S(t)\leqslant\rho_S^{\max}$. From Eq. (67), we then obtain $\overline{I_0}<e\min\{\gamma_1^{\uparrow},\gamma_2^{\uparrow}+\gamma_2^{\downarrow}\}t_p/t_r$. Note that for pulse lengths t_p, over which the dot spin evolves coherently, $t_p\gamma_1^{\uparrow}\lesssim 1$. Thus, by comparing the upper bound with Eq. (68), we see that for $\gamma_1^{\uparrow}<\gamma_2$ the background current $\overline{I_0}$ never becomes dominant.

Second, we consider $t_p\leqslant t\leqslant t_r$; i.e., the ESR field is switched off, and the dot state relaxes into its ground state $|\uparrow\rangle$. Making the reasonable assumption that the tunnel processes dominate the spin relaxation, $\gamma>W_{\uparrow\downarrow}$, we neglect $W_{\uparrow\downarrow}$ here. We then calculate the contribution for $t\geqslant t_p$ to the integral in Eq. (67) analytically and obtain

$$\overline{I}(t_p)-\overline{I_0}(t_p)=\frac{e}{t_r}\frac{\gamma_2^{\uparrow}+\gamma_2^{\downarrow}}{\gamma_1^{\downarrow}+\gamma_2^{\downarrow}}[\rho_{\downarrow}(t_p)+\rho_S(t_p)]\propto 1-\rho_{\uparrow}(t_p). \tag{68}$$

We now give a physical explanation for Eq. (68). We consider different tunneling events (after the pulse is switched off) and their contributions to the current, $\int_{t_p}^{t_r}dt\rho_S(t)$. Since we assume that at t_r the dot has relaxed into its ground state $|\uparrow\rangle$ and thus $\rho_S(t_r)=\rho_{\downarrow}(t_r)=0$, it is sufficient to consider only one pulse and to extend the upper integration limit to infinity. For the population $\rho_{\downarrow}(t_p)$ of state $|\downarrow\rangle$, the only allowed transition is $|\downarrow\rangle\rightarrow|S\rangle$ (neglecting again the intrinsic spin relaxation rate $W_{\uparrow\downarrow}$). Thus, eventually this population $\rho_{\downarrow}$ will be transfered to ρ_S and thus to the current. Note that sequences with $|S\rangle\rightarrow|\downarrow\rangle$ contribute to the current at a later time again, since the only possible decay into the ground state $|\uparrow\rangle$ involves $|S\rangle$. Therefore, concerning current contributions, we introduce the effective population $\rho_I=\rho_{\downarrow}+\rho_S$, which is the probability that at some later time an electron can still tunnel from the dot to lead 2. This ρ_I decays to state $|\uparrow\rangle$ with the rate $\gamma_S=\gamma_1^{\downarrow}+\gamma_2^{\downarrow}$, i.e., with the rate for the process $|S\rangle\rightarrow|\uparrow\rangle$. In total, integrating over $\rho_S(t)$ for $t>t_p$ yields $\int_0^{\infty}dt\rho_I(t_p)e^{-\gamma_S t}=[\rho_{\downarrow}(t_p)+\rho_S(t_p)]/\gamma_S$, and with Eq. (67) we immediately recover Eq. (68), as expected.

Next, we consider the case for spin-polarized leads. Here, no spin relaxation process due to tunneling occurs and the dot spin can only relax via intrinsic spin flips, given by the rate $W_{\uparrow\downarrow}$ (corresponding to the relaxation time T_1; we neglect $W_{\downarrow\uparrow}$ for $W_{\downarrow\uparrow}\ll W_{\uparrow\downarrow}$). Thus, we now consider the relaxation rate $W_{\uparrow\downarrow}$ instead of γ_S. The relaxation occurs only from $|\downarrow\rangle$ to $|\uparrow\rangle$; i.e., the roles of $|S\rangle$ and $|\downarrow\rangle$ are interchanged compared to the case for unpolarized leads considered above. The above argument now applies analogously by considering the (spin-polarized) current in lead 1, $I_1^{\uparrow}(t)=e\gamma_1^{\uparrow}\rho_{\downarrow}(t)$. We obtain

$$\overline{I^{\uparrow}}(t_p)\approx\frac{e}{t_r}\frac{\gamma_1^{\uparrow}}{W_{\uparrow\downarrow}}[1-\rho_{\uparrow}(t_p)], \tag{69}$$

with equality for $t_p\ll T_1$. We point out that for $\gamma_1^{\uparrow}\gg 1/T_1$, the (total) decoherence of the dot spin occurs much faster than its (intrinsic) relaxation. Then pulse lengths t_p, for which Rabi oscillations can be observed, are limited, $1/t_p\gtrsim V_{\downarrow\uparrow}>\gamma_1^{\uparrow}\gg W_{\uparrow\downarrow}$. In this case, the current contribution for $t\leqslant t_p$ can be neglected since it is suppressed by a factor of $t_pW_{\uparrow\downarrow}\ll 1$ compared to the contribution for $t\geqslant t_p$ [Eq. (69)]; see Fig. 9(c). Note that for spin-polarized leads, the relaxation time $W_{\uparrow\downarrow}^{-1}$ is usually much longer than for unpolarized leads, γ_S^{-1}; thus the required pulse repetition time $t_r>W_{\uparrow\downarrow}^{-1}$ might become very long. However, if one chooses a pulse repetition time $t_r=c/\gamma$, for $c>1$, and with the relevant relaxation rate γ, the current is proportional to $(1/t_r)\int_0^{\infty}dte^{-\gamma t}=1/c$, i.e., independent of γ. Thus, roughly speaking, the slow relaxation rate in the case of spin-polarized leads has no influence on the attainable maximum current since the decay from ρ_S and $\rho_{\downarrow}$ is much slower and thus per pulse there are more electrons passing the dot.

To conclude, we would like to emphasize again that the Rabi oscillations of the dot spin can be observed directly in the time domain by using pulsed ESR and measuring time-averaged currents (see Fig. 9). Observing Rabi oscillations also allows one to determine T_2 in the time domain; see Sec. IX B.[55]

XI. STM TECHNIQUES AND ESR

So far, we have considered a quantum dot coupled to leads. In this section, we would like to note that our description applies to more general structures showing Coulomb blockade behavior, such as Au nanoparticles[58] or C_{60} molecules,[59] which has been observed with STM techniques. This justifies that instead of a quantum dot, we now consider a localized surface state or an atom, molecule, or nanoparticle adsorbed on a substrate. This particle can then be probed with the STM tip by measuring the tunnel current through the particle. The current arises from electrons tunneling from the STM tip onto the particle and further tunneling, possibly through an insulating overlayer, into the bulk of the substrate.

In standard STM theory, the tunneling from the STM tip to the sample is treated pertubatively.[60] Evaluation of the golden rule matrix element, in the simplest model of a one-dimensional tunnel barrier, gives a tunneling amplitude, which is dominated by an exponential decay of the electronic wave function into the barrier; thus $t_l^{\sigma}\propto e^{-\kappa d}$ [cf. Eq. (13)], with $\kappa=\sqrt{2m\phi}$, tip-particle distance d, and barrier height ϕ (roughly given by the work function of the tip and sample). In particular, the perturbative description of STM is equivalent to our treatment of the tunneling Hamiltonian in first (sequential tunneling) order. Therefore, if the particle of interest shows Coulomb blockade behavior and has a spin-$\frac{1}{2}$ ground state, the master equation [Eqs. (16)–(21)] applies. Thus, using an ESR field, coherent Rabi oscillations and the T_2 time of the spin state of the particle can be accessed via

the current. Further, if spin-polarized tips and/or substrates are available (spin-polarized STM), such a particle can act as single spin memory with readout via current. Note that the tunneling rates from the STM tip into the particle can be controlled by changing the distance d; thus the total decoherence $V_{\downarrow\uparrow}$ [Eq. (15)], containing tunneling contributions, can be varied. This allows one, e.g., to vary the current linewidth $2V_{\downarrow\uparrow}$ (Sec. III B) and to suppress the Rabi spin flips for strong decoherence (Zeno effect, Sec. IX C). One apparent restriction of atomic or molecular systems is that it is difficult to apply a gate voltage to the particle, shifting its energy levels. However, the same effect can be achieved if the Fermi energies in the STM tip and the substrate can be shifted, such as by varying electron densities.

XII. DISCUSSION

We have shown how the single-spin dynamics of quantum dots can be accessed by current measurements. We have derived and analyzed coupled master equations of a quantum dot, which is tunnel coupled to leads, in the presence of an ESR field. The current through the dot in the sequential tunneling regime shows a new resonance peak (satellite peak) whose linewidth provides a lower bound on the single-spin decoherence time T_2. We have shown that also the cotunneling current has a resonant current contribution, giving access to T_2. The coherent Rabi oscillations of the dot spin can be observed by charge measurements, since they lead to oscillations in the time-dependent current and in the time-averaged current as function of ESR pulse length. We have shown how the ESR field can pump current through a dot at zero bias if spin-dependent tunneling or a spin inverter is available. We have discussed the concept of measuring a single spin via charge in detail. We have identified the measurement time of the dot spin via spin-polarized leads. Finally, we have noted that the concepts presented here are not only valid for quantum dots but also for ''real'' atoms or molecules if they are contacted with an STM tip.

ACKNOWLEDGMENTS

We thank C. Bruder, G. Burkard, S. De Franceschi, J.M. Elzerman, H. Gassmann, R. Hanson, A.V. Khaetskii, L.P. Kouwenhoven, M.N. Leuenberger, F. Marquardt, F. Meier, S. Oberholzer, P. Recher, D.S. Saraga, E.V. Sukhorukov, W.G. van der Wiel, and M.R. Wegewijs for discussions. We acknowledge support from the Swiss NSF, NCCR Nanoscience, DARPA, and ARO.

APPENDIX: STATIONARY CURRENT

Here, we give the various formulas for the stationary current through the dot in the sequential tunneling regime and in the presence of an ESR field. We have calculated the current by evaluating the stationary solution of the master equation (Sec. III) and with Eq. (22). For odd-to-even sequential tunneling, the spin $\uparrow$ polarized current in lead 2 is

$$
\begin{aligned}
I_2^{\uparrow} = e\gamma_2^{\uparrow}\Bigg(& \gamma_1^{\uparrow}\sum_{l,l'}(-1)^{l}\gamma_{l'}^{\downarrow}f_l(\Delta_{S\downarrow})f_{l'}(\Delta_{S\uparrow}) + \sum_{l}\frac{2W_{\omega}+W_{\uparrow\downarrow}+W_{\downarrow\uparrow}}{2}\{(-1)^{l}\gamma_1^{\uparrow}f_l(\Delta_{S\downarrow}) + \gamma_l^{\downarrow}[f_2(\Delta_{S\downarrow}) - f_l(\Delta_{S\uparrow})]\} \\
& - \sum_{l}\frac{W_{\uparrow\downarrow}-W_{\downarrow\uparrow}}{2}\{(-1)^{l}\gamma_1^{\uparrow}f_l(\Delta_{S\downarrow}) + \gamma_l^{\downarrow}[f_2(\Delta_{S\downarrow}) + f_l(\Delta_{S\uparrow}) - 2f_2(\Delta_{S\downarrow})f_l(\Delta_{S\uparrow})]\}\Bigg) \\
& \times\Bigg(\sum_{l,l'}\gamma_l^{\uparrow}\gamma_{l'}^{\downarrow}\{1-[1-f_l(\Delta_{S\downarrow})][1-f_{l'}(\Delta_{S\uparrow})]\} + \sum_{l,\sigma\neq\sigma'}(W_{\omega}+W_{\sigma'\sigma})\{\gamma_l^{\sigma}+\gamma_l^{\sigma'}[1-f_l(\Delta_{S\sigma})]\}\Bigg)^{-1}.
\end{aligned}
\tag{A1}
$$

The spin-$\downarrow$ polarized current $I_2^{\downarrow}$ is obtained from Eq. (A1) by exchanging all $\uparrow$ and $\downarrow$ in the numerator (the denominator remains unaffected by such an exchange). The currents in lead 1, $I_1^{\uparrow,\downarrow}$, are obtained from the formulas for $I_2^{\uparrow,\downarrow}$ by exchanging indices 1 and 2 and by a global change of sign. The charge current is $I_l=\Sigma_{\sigma}I_l^{\sigma}$ and is equal in both leads, $I=I_1=I_2$, due to charge conservation. For large Zeeman splitting, $\Delta_z > \Delta\mu, kT$, and around the spin satellite peak, $\mu_1 > \Delta_{S\downarrow} > \mu_2$ (see Sec. III A), we have $f_l(\Delta_{S\uparrow})=0$, and the current is

$$
\begin{aligned}
I = {} & e(W_{\omega}+W_{\downarrow\uparrow})[(\gamma_1^{\uparrow}\gamma_2^{\uparrow}+\gamma_1^{\uparrow}\gamma_2^{\downarrow})f_1(\Delta_{S\downarrow}) - (\gamma_1^{\downarrow}\gamma_2^{\uparrow}+\gamma_1^{\uparrow}\gamma_2^{\uparrow})f_2(\Delta_{S\downarrow})]\{(2\gamma^{\downarrow} - W_{\uparrow\downarrow} - W_{\omega})[\gamma_1^{\uparrow}f_1(\Delta_{S\downarrow}) + \gamma_2^{\uparrow}f_2(\Delta_{S\downarrow})] \\
& + 2(W_{\uparrow\downarrow}+W_{\downarrow\uparrow}+2W_{\omega})(\gamma^{\downarrow}+\gamma^{\uparrow})\}^{-1},
\end{aligned}
\tag{A2}
$$

for which we have given special cases in Eqs. (29), (30), and (31). Note that even at zero bias $\Delta\mu=0$, i.e., $f_1=f_2$, a current can be pumped through the dot, while the ESR field provides the required energy by exciting the spin state on the dot.[25] This requires spin-dependent tunneling rates, which break the symmetry between lead 1 and 2 and which determine the direction of the current, $\mathrm{sgn}(\gamma_1^{\uparrow}\gamma_2^{\downarrow} - \gamma_1^{\downarrow}\gamma_2^{\uparrow})$ [Eq. (A2)].

For completeness, we also give the results for even-to-odd sequential tunneling, as discussed in Sec. IV. By applying the replacements given in Sec. IV to Eq. (A1), we obtain the spin-$\downarrow$ polarized stationary current in lead 2,

$$I_2^{\downarrow}=e\gamma_2^{\downarrow}\Bigg(\gamma_1^{\downarrow}\sum_{l,l'}(-1)^l\gamma_{l'}^{\uparrow}f_l(\Delta_{\downarrow\bar{S}})[1-f_{l'}(\Delta_{\uparrow\bar{S}})]+\sum_l\frac{2W_\omega+W_{\uparrow\downarrow}+W_{\downarrow\uparrow}}{2}\{(-1)^l\gamma_1^{\downarrow}f_l(\Delta_{\downarrow\bar{S}})+\gamma_l^{\uparrow}[f_2(\Delta_{\downarrow\bar{S}})-f_l(\Delta_{\uparrow\bar{S}})]\}$$
$$-\sum_l\frac{W_{\uparrow\downarrow}-W_{\downarrow\uparrow}}{2}\{(-1)^l\gamma_1^{\downarrow}f_l(\Delta_{\downarrow\bar{S}})-\gamma_l^{\uparrow}[f_2(\Delta_{\downarrow\bar{S}})+f_l(\Delta_{\uparrow\bar{S}})-2f_2(\Delta_{\downarrow\bar{S}})f_l(\Delta_{\uparrow\bar{S}})]\}\Bigg)$$
$$\times\Bigg(\sum_{l,l'}\gamma_l^{\downarrow}\gamma_{l'}^{\uparrow}\{1-f_l(\Delta_{\downarrow\bar{S}})f_{l'}(\Delta_{\uparrow\bar{S}})\}+\sum_{l,\sigma\neq\sigma'}(W_\omega+W_{\sigma'\sigma})\{\gamma_l^{\sigma'}+\gamma_l^{\sigma}f_l(\Delta_{\sigma\bar{S}})\}\Bigg)^{-1}. \tag{A3}$$

*Electronic address: Hans-A.Engel@unibas.ch
†Electronic address: Daniel.Loss@unibas.ch

[1] J.M. Kikkawa and D.D. Awschalom, Phys. Rev. Lett. **80**, 4313 (1998).
[2] J.A. Gupta, D.D. Awschalom, X. Peng, and A.P. Alivisatos, Phys. Rev. B **59**, R10 421 (1999).
[3] M. Paillard, X. Marie, P. Renucci, T. Amand, A. Jbeli, and J.M. Gérard, Phys. Rev. Lett. **86**, 1634 (2001).
[4] F.G. Monzon and M.L. Roukes, J. Magn. Magn. Mater. **198**, 632 (1999).
[5] R. Fiederling M. Keim, G. Reuscher, W. Ossau, G. Schmidt, A. Waag, and L.W. Molenkamp, Nature (London) **402**, 787 (1999); Y. Ohno D.K. Young, B. Beschoten, F. Matsukura, H. Ohno, and D.D. Awschalom, *ibid.* **402**, 790 (1999).
[6] S. Lüscher, T. Heinzel, K. Ensslin, W. Wegscheider, and M. Bichler, Phys. Rev. Lett. **86**, 2118 (2001).
[7] T. Fujisawa, Y. Tokura, and Y. Hirayama, Phys. Rev. B **63**, R081304 (2001).
[8] J.A. Gupta, R. Knobel, N. Samarth, and D.D. Awschalom, Science **292**, 2458 (2001).
[9] D. Loss and D.P. DiVincenzo, Phys. Rev. A **57**, 120 (1998).
[10] G. Burkard, D. Loss, and D.P. DiVincenzo, Phys. Rev. B **59**, 2070 (1999).
[11] G. Burkard, H.-A. Engel, and D. Loss, Fortschr. Phys. **48**, 965 (2000).
[12] V. Privman, I.D. Vagner, and G. Kventsel, Phys. Lett. A **239**, 141 (1998).
[13] B.E. Kane, Nature (London) **393**, 133 (1998).
[14] A. Imamoğlu, D.D. Awschalom, G. Burkard, D.P. DiVincenzo, D. Loss, M. Sherwin, and A. Small, Phys. Rev. Lett. **83**, 4204 (1999).
[15] C.H.W. Barnes, J.M. Shilton, and A.M. Robinson, Phys. Rev. B **62**, 8410 (2000).
[16] R. Vrijen, E. Yablonovitch, K. Wang, H.W. Jiang, A. Balandin, V. Roychowdhury, T. Mor, and D. DiVincenzo, Phys. Rev. A **62**, 012306 (2000).
[17] J. Levy, quant-ph/0101026 (unpublished).
[18] X. Hu, R. de Sousa, and S. Das Sarma, Phys. Rev. Lett. **86**, 918 (2001).
[19] A. Abragam and B. Bleaney, *Electron Paramagnetic Resonance of Transition Ions* (Clarendon, Oxford, 1970).
[20] A.V. Khaetskii and Y.V. Nazarov, Phys. Rev. B **64**, 125316 (2001).
[21] J.P. Gordon and K.D. Bowers, Phys. Rev. Lett. **1**, 368 (1958).
[22] P.C. Hammel, Z. Zhang, G.J. Moore, and M.L. Roukes, J. Low Temp. Phys. **101**, 59 (1995); J.A. Sidles, J.L. Garbini, K.J. Bruland, D. Rugar, O. Züger, S. Hoen, and C.S. Yannoni, Rev. Mod. Phys. **67**, 249 (1995).
[23] L.P. Kouwenhoven, G. Schön, and L.L. Sohn, in *Mesoscopic Electron Transport*, Vol. 345 of *NATO Advanced Study Institute*, Series E, edited by L.L. Sohn, L.P. Kouwenhoven, and G. Schön (Kluwer Academic, Dordrecht, 1997).
[24] P. Recher, E.V. Sukhorukov, and D. Loss, Phys. Rev. Lett. **85**, 1962 (2000).
[25] H.-A. Engel and D. Loss, Phys. Rev. Lett. **86**, 4648 (2001).
[26] V.N. Golovach and D. Loss, cond-mat/0109155 (unpublished).
[27] T. Brandes, F. Renzoni, and R.H. Blick, Phys. Rev. B **64**, 035319 (2001).
[28] C.H. van der Wal, A.C.J. ter Haar, F.K. Wilhelm, R.N. Schouten, C.J.P.M. Harmans, T.P. Orlando, S. Lloyd, and J.E. Mooij, Science **290**, 773 (2000).
[29] C. J. P. M. Harmans (private communication).
[30] R.H. Blick, V. Gudmundsson, R.J. Haug, K. von Klitzing, and Karl Eberl, Phys. Rev. B **57**, R12 685 (1998).
[31] M. Dobers, K. von Klitzing, J. Schneider, G. Weimann, and K. Ploog, Phys. Rev. Lett. **61**, 1650 (1988).
[32] S. Tarucha D.G. Austing, T. Honda, R.J. van der Hage, and L.P. Kouwenhoven, Phys. Rev. Lett. **77**, 3613 (1996).
[33] One distinguishes between $\mu_{\rm dot}$, which is the energy required for an electron of the lead to tunnel onto the dot, and the addition energy $E_{\rm add}=\mu_{\rm dot}(N+1)-\mu_{\rm dot}(N)=e^2/C+\varepsilon_{N+1}^{\sigma}-\varepsilon_N^{\sigma}$. When lead l provides enough energy such that an electron can tunnel onto the dot $[\mu_l>\mu_{\rm dot}(N)]$, the addition energy is the extra energy the lead must provide such that an *additional* electron can tunnel onto the dot as well, $\mu_l'=\mu_l+E_{\rm add}>\mu_{\rm dot}(N+1)$. The current as function of the gate voltage shows sequential tunneling peaks at $\mu_{\rm dot}(N)$. Thus, $E_{\rm add}$ is proportional to the distance of two subsequent peaks.
[34] E. Fick and G. Sauermann, *The Quantum Statistics of Dynamic Processes*, Springer Series in Solid State Sciences Vol. 86 (Springer, Berlin, 1990).
[35] At this point, one usually makes a secular approximation (Ref. 36) by neglecting terms in $M^{\rm I}$ [Eq. (8)] that rapidly oscillate with the energy difference of different states on the dot. However, it is noteworthy that for the system considered here, no such terms appear and thus no such secular approximation is required.
[36] K. Blum, *Density Matrix Theory and Applications* (Plenum, New York, 1996), Chap. 8.
[37] B. Thimmel, P. Nalbach, and O. Terzidis, Eur. Phys. J. B **9**, 207 (1999); F. Bloch and A. Siegert, Phys. Rev. **57**, 522 (1940).
[38] PAT effects are due to the electric rf field component (see Sec. II A) and thus are less sensitive to changes in B_z, compared to the magnetic ESR effects described here.

[39] It has been suggested to test the functionality of spin filtering by an electron interference experiment with an Aharonov-Bohm (AB) ring, with one dot in each arm of the ring (Ref. 61). On the one hand, if both dots allow the same spin to pass, the flux enclosed by the electron moving through the upper as well as through the lower arm will lead to interference and the resulting AB oscillations are observable in the current. On the other hand, if the dots filter out different electron spins—say, all spin-↑ electrons go through the upper arm while all spin-↓ electrons go through the lower arm of the ring—no magnetic flux is enclosed by either spin current and thus no interference occurs. However, there is still a leakage (cotunneling) current of the opposite spin through the spin filters (Ref. 24), thus there is still a small current contribution showing AB oscillations.

[40] P. Recher, E.V. Sukhorukov, and D. Loss, Phys. Rev. B **63**, 165314 (2001).

[41] E. Merzbacher, *Quantum Mechanics*, 3rd ed. (Wiley, New York, 1998), Chap. 20.

[42] For nonmagnetic photon-assisted pumps see, e.g., Ref. 23 and B.L. Hazelzet, M.R. Wegewijs, T.H. Stoof, and Yu.V. Nazarov, Phys. Rev. B **63**, 165313 (2001).

[43] Generically this is satisfied. However, if there is no complete basis of eigenvectors of $\mathcal{M}$, there is power law admixture. For instance, for $\Delta_\perp = \Sigma_W - V_{\downarrow\uparrow}$, the last two eigenvalues, $\lambda_\pm$, in Eq. (47) are degenerate. Then, the time evolution of $\boldsymbol{\rho}_{\mathrm{D}}$ can contain terms proportional to $te^{\lambda_\pm t}$.

[44] D.V. Averin and Yu. V. Nazarov, in *Single Charge Tunneling*, Vol. 294 of *NATO Advanced Study Institute, Series B*, edited by H. Grabert and M.H. Devoret (Plenum, New York, 1992).

[45] H. Schoeller and G. Schön, Phys. Rev. B **50**, 18 436 (1994); J. König, H. Schoeller, and G. Schön, *ibid.* **58**, 7882 (1998).

[46] E.V. Sukhorukov, G. Burkard, and D. Loss, Phys. Rev. B **63**, 125315 (2001).

[47] D. Loss and E.V. Sukhorukov, Phys. Rev. Lett. **84**, 1035 (2000).

[48] M. Ciorga, A.S. Sachrajda, P. Hawrylak, C. Gould, P. Zawadzki, S. Jullian, Y. Feng, and Z. Wasilewski, Phys. Rev. B **61**, R16 315 (2000).

[49] M.J.M. de Jong, Phys. Rev. B **54**, 8144 (1996).

[50] Ya.M. Blanter and M. Büttiker, Phys. Rep. **336**, 1 (2000).

[51] M.H. Devoret and R.J. Schoelkopf, Nature (London) **406**, 1039 (2000).

[52] For the measurement process in Josephson qubits, see Y. Makhlin, G. Schön, and A. Shnirman, Phys. Rev. Lett. **85**, 4578 (2000).

[53] Note that by using transport involving many states of the dot, the readout current could be increased and thus the readout time further decreased. Further, if instead resonant tunneling is considered, e.g., into an SET device, faster readout could be achieved.

[54] Note that in general $I_1(t) \neq I_2(t)$, since charge can accumulate on the dot for some typical time, which is limited from above by the inverse tunneling rates. Here, charge accumulation occurs with the period of the Rabi oscillations Δ_x^{-1}.

[55] An alternative application of pulsed ESR for measuring T_2 is spin echo, where a well-defined sequence of pulses is applied to cancel the effect of dephasing (Refs. 19,21 and 62). At the end of the sequence, the dot spin (in the σ_z basis) can be measured by one of the techniques discussed in Secs. VIII, IX A, and X. Here, spin echo compensates for dephasing of an array of quantum dots in an inhomogeneous magnetic field B_z or in time series measurements (on a single dot), where the magnetic field B_z fluctuates in time. More care must be taken for inhomogeneities in the g factor (Rabi frequency Δ_x), since then a pulse does not rotate the spin by an equal angle for every dot. To compensate this, one could, e.g., use Carr-Purcell-Meiboom-Gill pulse sequences (Ref. 62).

[56] A. Peres, *Quantum Theory* (Kluwer Academic, Amsterdam, 1993).

[57] We note that similar concepts have been used in recent experiments (Ref. 63), however with a separation of time scales, $T_\Omega, t_p \ll \gamma^{-1}$. We show here that such concepts can be applied more generally for regimes where $T_\Omega, t_p \lesssim \gamma^{-1}$.

[58] C. Schönenberger, H. van Houten, and H.C. Donkersloot, Europhys. Lett. **20**, 249 (1992).

[59] D. Porath and O. Millo, J. Appl. Phys. **81**, 2241 (1996).

[60] C.J. Chen, *Introduction to Scanning Tunneling Microscopy* (Oxford University Press, New York, 1993).

[61] J.A. Folk, R.M. Potok, A.C. Johnson, S.M. Cronenwett, C.M. Marcus, W.G. van der Wiel, and L.P. Kouwenhoven, APS March Meeting (2001), C25.4 (unpublished).

[62] C.P. Slichter, *Principles of Magnetic Resonance* (Springer, Berlin, 1990).

[63] Y. Nakamura, Yu.A. Pashkin, and J.S. Tsai, Nature (London) **398**, 786 (1999).